University of Stuttgart

Institute for Theoretical Physics III

Master Thesis

Quantum Phases of Water Molecules in Nano-cavities

Luka Jibuti

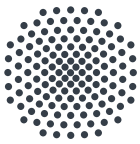

Universität Stuttgart

Supervised by
Prof. Dr. H. P. Büchler

Secondary Corrector
Apl. Prof. Dr. J. Main

Statutory Declaration

I herewith formally declare that I have written and submitted the thesis independently. I did not use any outside support except for the quoted literature.

I clearly marked and separately listed all of the literature and all necessary sources which I used for the thesis.

Stuttgart, October 20, 2018. Luka Jibuti

Contents

List of Figures

Acknowledgements

I would like the express my immeasurable gratitude towards my supervisor Prof. Hans Peter Büchler. Working on this thesis and alongside his group - ITP3 - I have gained a lot of experience and knowledge. I would like to thank Nicolai Lang and Stephan Humeniuk for hours of helpful discussions. All in all, I want to thank the Whole *Institute of Theoretical Physics III* group for their support.

I also would like to thank my second supervisor Prof. Jörg Main, for helpful discussions over my topic and Prof. Martin Dressel, for interesting and important discussion about my topic and about beryl minerals.

Introduction

Water molecule is the most abundant molecule on Earth [1]. H_2O, most commonly appearing in liquid form (but also in gas and solid state), consists of two hydrogen atoms and an oxygen atom. Eight positive charges in oxygen nucleus attract all electrons from hydrogen atom, leading to a deficiency of negative charge around hydrogen atoms. On the contrary, the excess negative charge is situated close to oxygen atom making it partially negatively charged. Hence the surfaces of negative and positive charges appear making the water molecule polar. Even though it is studied extensively, water molecules shows interesting properties when put into nano-cages (or nano-cavities) due to *hydrogen bonding*.

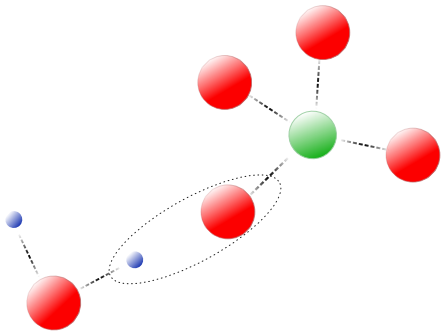

Figure 1: Water molecule (lower left) and SiO_4(upper right). With red bubbles we represent oxygen atoms, with blue ones - hydrogen atoms and with the green bubble we show silicon atom. When one of the O-H bonds from the water molecules points directly at a near oxygen atom the attraction becomes very strong.

Since the hydrogen atom in water molecule is positively charged, it will interact with atoms of having valence electrons (thus, with more negatively charged atoms), forming hydrogen bonds. (see figure (3))).

Even though water molecules has numerous properties, we will focuse on these two and use them extensively throughout this thesis.

We will explore water molecules confined in the nano-cavities of beryl crystal. Beryl is a mineral, its chemical formula being $Be_3Al_2Si_6O_{18}$, composed of beryllium aluminum silicate and belongs to the family of the hexagonal crystals. In the *Figure* (2) we see a horizontal cut of the general three-dimensional crystal. the layer shown here is perpendicular to crystallography c-axis. The beryl crystal consists of SiO_4 (represented in the figure as yellow triangles), forming a six-membered rings (or as we refer to them as honeycomb structures) creating nano-cavities. These nano-cavities sit on top of each other forming channels along the c-axis. In this channels there are bottlenecks of diameter 2.1 Å, where one can place Alkali ions (Na or K) [2], in between two cavities of diameter 5.1 Å [2], where different molecules (H_2O or CO_2) cam be embedded [3]. Since the approximate diameter of water molecule is 2.75 Å it is possible to place single water molecules inside the nano-cavity. Water molecules, rotating inside the cavities form a *hydrogen bonds* between oxygen atoms of SiO_4. Since there are six oxygen atoms in the ring forming the

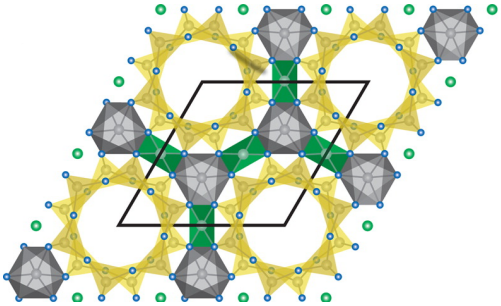

Figure 2: A layer of the beryl crystal [2]. *Yellow* triangles represent SiO_4 molecules. The nano-cavities created by this rings of SiO_4 molecules can host *single* water molecules.

honeycomb structure, the interaction potential has to have the following symmetry property:

$$U\left(\phi + \frac{\pi}{3}\right) = U(\phi) \quad , \tag{1}$$

where ϕ is the rotational angle of the dipole moment of the water molecule. The strength of the potential is determined by the strength of the **O-H** bonds between water molecule and SiO_4.

The *goal* of this research is to do a theoretical investigation of the phase diagram of water molecules embedded in the nano-cavities of beryl crystal. For simplicity, we will treat water molecules as *point particles* having the dipole moment $\vec{d}$. Interaction between two dipoles **i** and **j** (see *Figure* (3)), distance between each other being $|\vec{R}_{ij}| >> |\vec{r}_i|, |\vec{r}_j|$, where $\vec{r}$ is the distance between opposite charges in a dipole, can be written as follows:

$$V_{dd}^{ij} = \frac{1}{4\pi\epsilon_0 |\vec{R}_{ij}|^3} \left\{ \vec{d}_i \cdot \vec{d}_i - 3\frac{(\vec{R}_{ij} \cdot \vec{d}_i)(\vec{R}_{ij} \cdot \vec{d}_j)}{|R_{ij}|^2} \right\} \quad . \tag{2}$$

Here $\epsilon_0 \approx 8.85 \times 10^{-12} Fm^{-1}$ is the vacuum permittivity. $\vec{d} = -e\vec{r}$ is the dipole moment of a particle.

We will investigate quantum phase transitions appearing in dipole systems in one, two and three-dimensions and describe the phase diagram for all these situations. The most general form

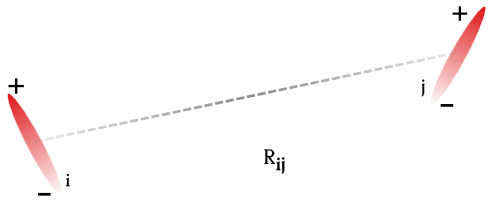

Figure 3: Two dipoles, distance between them being $\vec{R}_{i,j}$, interacting with each other. The green dots represent positively charged protons, whereas red dots represents negatively charged electrons. $\vec{r}_i(\vec{r}_j)$ is the distance between the proton and the electron of dipole "i"("j"). It is assumed that $|\vec{R}_{ij}| >> |\vec{r}_i|, |\vec{r}_j|$.

of the Hamiltonian for such systems can be written as follows:

$$\hat{H} = \sum_i^N \hat{H}_m + \frac{1}{2}\sum_{i,j} V_{dd}^{i,j} + U(\theta) \quad . \tag{3}$$

Here $\hat{H}_m$ is the kinetic energy of the system, $V_{dd}^{m,n}$ and $U(\theta)$ are given in *eq.*(2) and *eq.*(1). Because of the long range nature of the dipole-dipole interaction, calculations for higher-dimensional systems become complicated. Hence, in order to understand the physical aspects of multi-dimensional systems, we have to start our investigation with the simplest model.

The starting point, ***Chapter*** 2, of the thesis is the investigation of the phase diagram for identical dipoles forming *one-dimensional chain*. Initially, we will assume that the six-fold potential $U(\phi)$ is *weak* enough, that we can neglect its effects on the system. Obtaining the classical limit (*section* 2.1) for such a system, we will write the mean-field potential (taking into account the configuration in classical limit) and write the Schrödinger equation (*section* 2.2). Obtaining the self-consistent equation we will find the critical point, where the quantum phase transition from highly disordered to ordered state occurs, and also we will be able to describe the phase diagram. Afterwards, we will increase the strength of the six-fold potential such, that we will be able use the tight-binding approach. Assuming the mean-field potential as a perturbation, we will use the perturbation theory to obtain a new value for the critical point D_{crit}. We will also show that the general phase diagram will remain the roughly the same.

As we move to higher dimensions, the situation becomes more complicated due to the long range nature of the dipole-dipole interaction. during the research we were able to deduce that the intuition that we had for the one-dimensional chain was completely impractical for higher dimensions.

We start dealing with the two-dimensional system by discussing a "*toy model*": quadratic lattice. Even though this is not the true lattice that water molecules create when they are nested in the beryl crystal, we believe that the derivation of the Hamiltonian and investigation of the phase diagram of such a system will be of great importance and will provide a valuable preliminary background towards the investigation of the real system: triangular lattice.

In ***Chapter* 3** we begin our investigation of the quadratic lattice by writing the classical form of the dipole-dipole interaction. Observing three different configurations: *polarized* (3.1.1), *striped* (3.1.2) and *checkerboard* (3.1.3), which have the potential to have the lowest energy, and calculating the potential energy for each system we will be able obtain the *ground state* configuration. Using this knowledge, we will write the potential (per particle) in the *mean-field* approximation (3.1.4) and examine the behavior of the system when the fluctuations created by the introduction of the kinetic energy are strong. Solving the Schrödinger equation and obtaining the self-consistent equation we are able to obtain the critical point, where the phase transition occurs. Knowing the overall properties of the phase diagram we will increase the strength of the six-fold potential and observe the changes in the phase diagram introduced by it.

The work done on the square lattice gives us a necessary background to start our investigation of the true lattice appearing in the beryl crystal. As depicted in the Figure (), water molecules inserted in the nano-cavities of the beryl crystal form a triangular lattice. Initially we assume that the lattice is ideal (every site is occupied with a single water molecule). Using the results obtained for the quadratic lattice we will examine (see *Section* 3.2 of ***Chapter*** 3) two different combinations appearing in triangular lattice. These are: *polarized* (3.2.1), *striped* (3.2.2). Writing down the dipole-dipole interaction and comparing the potential energies (per particle) for these two configurations, we will be able to find the *ground state* configuration. Knowing this, we will write the mean-field potential and derive the Schröringer equation. Obtaining the self-consistent equation we will find the critical point, where the quantum phase transitions occurs. We will also find that the ground state of dipoles in triangular lattice has a *global* $O(2)$ rotational symmetry.

In the coarse of the research we asked ourselves: what would happen to the system (either globally or locally) if the lattice was not ideal, meaning there could exist defects or *deficiencies* in the system. In order to observe the changes of the symmetry of the system in the ground state we will remove a single dipole from the lattice (3.3). Letting the system relax to a "*new*" ground state we will observe that the local symmetry is disturbed.

Investigation, done in ***Chapter*** 4, of the ground state properties of dipoles in the three-dimensional system is trivial knowing the ground state properties of dipoles in the two-dimensional triangular lattice. One has to picture a three-dimensional system as layers of triangular lattices put on top of each other. Hence, knowing the ground state orientation of one of the layers from ***Chapter*** 3, we will able to obtain the ground state ordering of the neighboring layers. Moreover, we find that the ground state configuration for the three-dimensional system is different from the two-dimensional one.

We will start our thesis with the short introduction to *Hartree-Fock Approximation For Bosonic System*, which will lay a helpful background of the upcoming analysis.

Chapter 1

Introduction to Hartree-Fock Approximation For Bosonic System

Let us assume that the Hamiltonian for the system of N particles is given as follows:

$$\hat{H} = \sum_{m}^{N} \hat{T}(\vec{x}_m) + \frac{1}{2} \sum_{m,n}^{N} V(\vec{x}_m, \vec{x}_n) \quad . \tag{1.1}$$

Here $\hat{T}(\vec{x}_m)$ is the kinetic energy operator for particle m, and $V(\vec{x}_m, \vec{x}_n)$ is the pair interaction potential. In the second summation we assume that $m \neq n$. Let us introduce the following anzatz for the wave-function of the system:

$$\psi(\vec{x}_1, \vec{x}_2, ..., \vec{x}_N) = \phi(\vec{x}_1)\phi(\vec{x}_2)...\phi(\vec{x}_N) \tag{1.2}$$

We assume that the individual wave-functions describing individual particles are normalized. Let us calculate the mean value of the total Hamiltonian:

$$\langle\psi| H |\psi\rangle = \langle\psi| \sum_{m}^{N} \hat{T}(\vec{x}_m) |\psi\rangle + \frac{1}{2} \langle\psi| \sum_{m,n}^{N} V(\vec{x}_m, \vec{x}_n) |\psi\rangle \quad . \tag{1.3}$$

For the first term we will obtain:

$$\begin{aligned} \langle\psi| \sum_{m}^{N} \hat{T}(\vec{x}_m) |\psi\rangle &= \sum_{m}^{n} \langle\phi(\vec{x}_m)| \hat{T}(\vec{x}_m) |\phi(\vec{x}_m)\rangle \\ &= \sum_{m}^{N} \int d\vec{x}_m \phi^*(\vec{x}_m) \hat{T}(\vec{x}_m) \phi(\vec{x}_m) \quad . \end{aligned} \tag{1.4}$$

for the interaction term we can write:

$$\begin{aligned} \langle\psi| \sum_{m,n}^{N} V(\vec{x}_m, \vec{x}_n) |\psi\rangle &= \sum_{m,n}^{N} \langle\phi(\vec{x}_m), \phi(\vec{x}_n)| V(\vec{x}_m, \vec{x}_n) |\phi(\vec{x}_m), \phi(\vec{x}_n)\rangle \\ &= \sum_{m,n} \int \int d\vec{x}_m d\vec{x}_n \phi^*(\vec{x}_m) \phi^*(\vec{x}_n) V(\vec{x}_m . \vec{x}_n) \phi(\vec{x}_m) \phi(\vec{x}_n) \quad . \end{aligned} \tag{1.5}$$

Plugging eq.(1.4) and eq.(1.5) into the eq.(1.3) for mean value of Hamiltonian, we will obtain:

$$\begin{aligned} \langle\psi|\, H\, |\psi\rangle &= \sum_{m}^{N} \int d\vec{x}_m \phi^*(\vec{x}_m) \hat{T}(\vec{x}_m) \phi(\vec{x}_m) \\ &+ \frac{1}{2} \sum_{m,n} \int\int d\vec{x}_m d\vec{x}_n \phi^*(\vec{x}_m)\phi^*(\vec{x}_n) V(\vec{x}_m.\vec{x}_n)\phi(\vec{x}_m)\phi(\vec{x}_n) \quad . \end{aligned} \tag{1.6}$$

Applying the variational principle to the obtained value of $\langle\psi|\, H\, |\psi\rangle$, we will end up with the following one particle equation:

$$\sum_{m}^{N} \left\{ \hat{T}(\vec{x}_m) + \frac{1}{2} \sum_{n} \langle\phi(\vec{x}_n)|\, V(\vec{x}_m, \vec{x}_n)\, |\phi(\vec{x}_n)\rangle \right\} \phi(\vec{x}_m) = \sum_{m} E_m \phi(\vec{x}_m) \tag{1.7}$$

Hence, we obtained a series of **N** differential equations describing the system. The Schrödinger equation for a single particle **m** will be:

$$\hat{T}(\vec{x}_m)\phi(\vec{x}_m) + \frac{1}{2} \sum_{n} \tilde{V}_{m,n} \phi(\vec{x}_m) = E_m \phi(\vec{x}_m) \quad , \tag{1.8}$$

where:

$$\tilde{V}_{m,n} = \langle\phi(\vec{x}_n)|\, V(\vec{x}_m, \vec{x}_n)\, |\phi(\vec{x}_n)\rangle \tag{1.9}$$

Eq.(1.8) will be very useful in the upcoming chapters.

As said in the introduction, we start our investigation with the one-dimensional chain of identical dipoles.

Chapter 2

One-dimensional Chain of Identical Dipoles

Let us arrange **N** dipoles such, that they form a one-dimensional chain. This structure is depicted in Figure (2.1). We will assume that once the dipole is placed in the lattice site it cannot move anywhere. But we allow each dipole to *rotate* around the y-axis. Also, we assume that the distance between neighboring dipoles is $r_{i,i\pm1} = a$.

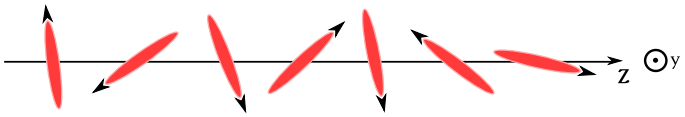

Figure 2.1: One-dimensional chain of identical dipoles. The distance between two neighboring dipoles is constant: $r_{i,i]pm1} = a$. "Y" axis is perpendicular to the paper. We assume that dipoles can only rotate in "$X - Z$" surface.

As seen in *eq.* (2), each pair of dipoles, for example dipoles **i** and **j** interact with each other via dipole-dipole interaction. Here we write a simplified version of that interaction:

$$V_{dd}^{i,j} = \frac{1}{4\pi\epsilon_0 z_{i,j}^3}\Big(\vec{d}_i \cdot \vec{d}_j - 3(\vec{e}_{i,j} \cdot \vec{d}_i)(\vec{e}_{i,j} \cdot \vec{d}_j)\Big) \quad , \tag{2.1}$$

where $\epsilon_0 \approx 8.85 \times 10^{-12} Fm^{-1}$ is the vacuum permittivity, and $\vec{e}_{i,j}$ is a unit vector. Notice that since we are in one-dimension we have omitted a vector sign for $z_{i,j}$. We will attempt to write the dipole-dipole interaction in terms of angles of dipoles with regards to z-axis. Using the spherical coordinates and remembering the restriction that we applied for the dipoles, the first scalar product in *eq.*(2.1) can be written as follows:

$$\vec{d}_i \cdot \vec{d}_j = |d|^2\Big(\cos(\theta_i)\cos(\theta_j) - \sin(\theta_i)\sin(\theta_j)\Big) = |d|^2\cos(\theta_i - \theta_j) \quad . \tag{2.2}$$

For the second scalar product between the unit vector and the dipole moment, we will have:

$$(\vec{e}_{i,j} \cdot \vec{d}_i)(\vec{e}_{i,j} \cdot \vec{d}_j) = |d|^2\cos(\theta_i)\cos(\theta_j) \quad . \tag{2.3}$$

Plugging eq.(2.2) and eq.(2.3) into eq.(2.1) we will obtain:

$$\begin{aligned} V_{dd}^{i,j} &= \frac{|d|^2}{4\pi\epsilon_0 z_{i,j}^3}\Big(\cos(\theta_i - \theta_j) - 3\cos(\theta_i)\cos(\theta_j)\Big) \\ &= \frac{C_{dd}}{4\pi|j-i|^3}\Big(\sin(\theta_i)\sin(\theta_j) - 2\cos(\theta_i)\cos(\theta_j)\Big) \quad . \end{aligned} \tag{2.4}$$

Here $C_{dd} = |d|^2/\epsilon_0 a^3$ is the dipole-dipole interaction strength. The potential energy of dipole **i** due to interactions between all remaining **N-1** dipoles in the system is a sum over all values of **j** except $j = i$. Thus we can write:

$$V_{dd}^{i} = \frac{C_{dd}}{4\pi} \sum_{j \neq i} \frac{1}{|j-i|^3} \Big(\sin(\theta_i)\sin(\theta_j) - 2\cos(\theta_i)\cos(\theta_j) \Big) \quad . \tag{2.5}$$

Before we write the total Hamiltonian of the system let us look at the kinetic energy (**T**) of the system. We have to remember that dipoles have only one degree of freedom: thy can rotate around the y-axis. In general the kinetic energy in spherical coordinates can be written:

$$\hat{T} = -\frac{\hbar^2}{2\mu}\nabla^2 = -\frac{\hbar^2}{2\mu}\left\{ \frac{1}{r}\frac{\partial^2}{\partial r^2} + \frac{1}{r^2\sin(\phi)}\frac{\partial}{\partial\phi}\left(\sin\phi\frac{\partial}{\partial\phi}\right) + \frac{1}{r^2\sin^2\phi}\frac{\partial^2}{\partial\theta^2} \right\} \quad ,$$

where μ is the reduced mass of the dipole (for our case μ is the reduced mass of the water molecule) and r is the length of the dipole moment. Since r and ϕ are considered constant ($\phi = \pi/2$), the kinetic energy operator can be simplified. Thus the Hamiltonian for the Total system will be as follows:

$$\hat{H} = -\frac{\hbar^2}{2I}\sum_i \frac{\partial}{\partial\theta_i^2} + \frac{C_{dd}}{8\pi}\sum_i\sum_{j\neq i}\frac{1}{|j-i|^3}\Big(\sin(\theta_i)\sin(\theta_j) - 2\cos(\theta_i)\cos(\theta_j)\Big) \quad . \tag{2.6}$$

Knowing this, in the beginning we will look at the system in the classical limit: we will assume that the kinetic energy (**T**) is smaller than the potential energy (**V**) such, that the fluctuations created by the kinetic energy can be neglected.

From here on, we will do all calculations assuming that the system is in *thermodynamic limit*, meaning that the total number of dipoles $N \to \infty$.

2.1 Classical Limit: Polarized and Striped Configurations

Let us first look at the classical picture (or the classical limit) and try to obtain the *minimum energy configuration* using the potential energy in *eq.*(2.5). Let us assume that for some reason the system chooses the *polarized* configuration, meaning that for all values **j** (including **j** = **i**): $\theta_j = \theta$. Then V_{dd}^i in *eq.*(2.5) will become:

$$V_{dd}^i = \frac{C_{dd}}{4\pi} \sum_{j \neq i} \frac{1 - 3\cos^2(\theta)}{|j-i|^3} \quad . \tag{2.7}$$

Notice here that summation over **j** takes both negative and positive values of **j**. Since we are dealing with the thermodynamic limit ($N \to \infty$), we can argue that it becomes *irrelevant* which dipole **i** we are talking about. If our system was finite, calculations of the potential energy, and thus the calculations of the ground state configuration, would strongly depend on the location of the dipole in the system: on the *edges* of the system the behavior of the dipoles would be vastly different from that of the dipoles placed in the *center* of the system. Since the system is infinite, every dipole will share the same properties. Thus, for simplicity we can assume that $i = 0$ and re-write the potential in the following way:

$$V_{dd}^0 = \frac{C_{dd}}{2\pi} \sum_{j>0} \frac{1 - 3\cos^2(\theta)}{j^3} = \big(1 - 3\cos^2(\theta)\big) \frac{C_{dd}}{2\pi} \zeta(3) \quad , \tag{2.8}$$

where $\zeta(n)$ is the Riemann zeta function (see Appendix B).

In *eq.*(2.8) we used the following property:

$$\sum_{j<0} + \sum_{j>0} = 2 \sum_{j>0} \quad .$$

Let us minimize the potential in *eq.*(2.8). The first derivative with regards to θ will give:

$$\frac{d}{d\theta} V_{dd}^0 = \frac{3C_{dd}}{2\pi\zeta(3)} \sin(2\theta) \quad . \tag{2.9}$$

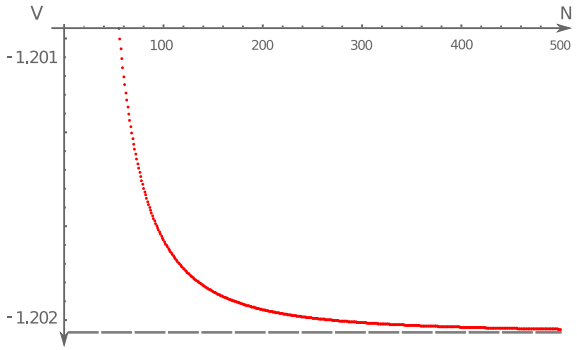

Figure 2.2: V_{dd}^0 (per particle) for polarized ordering as a function of number of dipoles N. Here we let $\frac{C_{dd}}{2\pi} = 1$.

Thus we will have the following solutions:

$$\theta = n\pi; \quad \text{or} \quad \theta = n\frac{\pi}{2} \quad , \tag{2.10}$$

where $n = \{0, 1, 2, ...\}$. Doing the second order derivative of V_{dd}^0, we will arrive at:

$$\frac{d^2}{d\theta^2} V_{dd}^0 = \frac{3C_{dd}}{\pi\zeta(3)} \cos(2\theta) \quad . \tag{2.11}$$

Plugging the results in *eq.*(2.11) we will have:

$$\left.\frac{d^2}{d\theta^2}V_{dd}^0\right|_{\theta=n\pi} = \frac{3C_{dd}}{\pi}\zeta(3) > 0 \quad \text{and} \quad \left.\frac{d^2}{d\theta^2}V_{dd}^0\right|_{\theta=n\frac{\pi}{2}} = -\frac{3C_{dd}}{\pi}\zeta(3) < 0 \quad , \tag{2.12}$$

Hence, we see that if all dipoles are *polarized* with polarization angle θ, the minimization of the energy requires that $\theta = n\pi$. The potential for $\theta = 0$ can be written as follows:

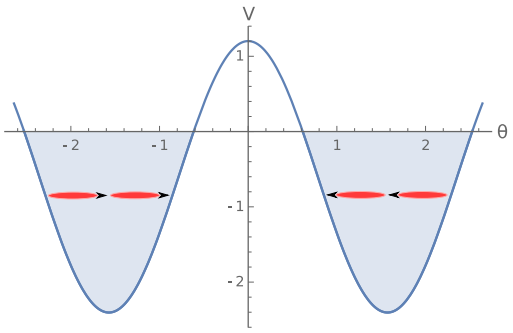

Figure 2.3: V_{dd}^0 (per particle) for polarized ordering as a function of number of dipoles polarization angle θ. Here we let $\frac{C_{dd}}{2\pi} = 1$.

$$V_{dd}^{Pol} = -\frac{C_{dd}}{\pi}\zeta(3) \approx -1.202\frac{C_{dd}}{\pi} \quad . \tag{2.13}$$

In the figure bellow we can see how the system is ordered in classical limit. The *Figure* (2.2) shows

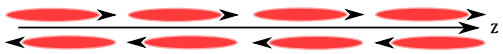

Figure 2.4: Polarized ordering of the dipoles in one-dimensional chain.

the minimum value of potential V_{dd}^0 (per particle) as a function of N. In the figure we assume that $C_{dd}/2\pi = 1$. Notice the *Figure* (2.3). Here we have plotted the potential energy (per particle) for the polarized configuration. We see two minimums appearing in the system. The *left* is for $\theta = 0$ (during plotting we have shifted θ with $-\pi/2$) and the *right* is for $\theta = \pi$. Since these two configurations have exactly the same energy, we argue that we have a *spontaneous symmetry breaking* in the system: the system will choose either $\theta = 0$ or $\theta = \pi/2$ configuration.

One can also think about other ordering that might appear in the system. In particular, the *striped* ordering (see *Figure* (2.5)). Mathematically it can be defined as follows:

$$\theta_{i+m} = \theta_i + m\pi \quad \rightarrow \quad \cos(\theta_{i+m}) = (-1)^m\cos(\theta_i) \quad . \tag{2.14}$$

For this case the total interaction potential V_{dd}^0 will become (see *eq.*(2.5)):

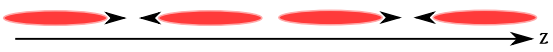

Figure 2.5: Striped ordering of the dipoles in one-dimensional chain.

$$V_{dd}^0 = \frac{C_{dd}}{2\pi}\sum_{j>0}(-1)^j\frac{1-3\cos^2(\theta)}{j^3} \quad . \tag{2.15}$$

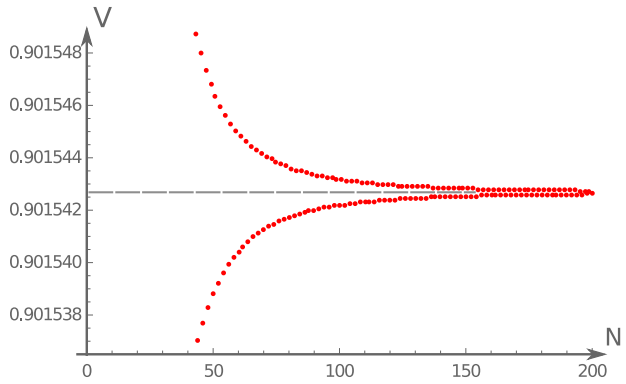

Figure 2.6: V_{dd}^0 for striped ordering as a function of number of dipoles N. Here we let $\frac{C_{dd}}{2\pi a^3} = 1$

Doing the energy minimization (same steps that we did above) we find that minimum energy requires that $\theta = n\pi$. The potential for $\theta = 0$ is as follows:

$$V_{dd}^{Str} = \frac{C_{dd}}{2\pi} \sum_{j>0} (-1)^j \frac{1}{j^3} \approx -0.902 \frac{C_{dd}}{2\pi} \quad . \tag{2.16}$$

Figure (2.6) shows the minimum value potential for the stripe orientation (per particle) as a function of N. In the figure we assume that $C_{dd}/2\pi = 1$.

2.2 The Mean-field Approximation

In the previous section we have obtained that in the classical limit ($\mathbf{T} < \mathbf{V}$) all dipoles forming a one-dimensional chain are polarized along (or anti-parallel) to z-axis. Let us now increase the kinetic energy. By doing so all dipoles will start to *oscillate* around the minimum energy configuration. As the kinetic energy of the each dipole further increases, the oscillations become stronger and we have to observe that the ordering established in classical limit gets *destroyed*, indicating the existence of the quantum phase transition. In order to observe this transition, we will do the following. We will write the potential using the mean-field approximation (see ***Chapter* 1**) and assuming that the kinetic energy is larger than the potential energy we will write and solve the Schr"odinger equation. First we will attempt to write the dipole-dipole interaction in the mean-field approximation. Using *eq.*(1.7) we will have:

$$\langle\psi_j| V_{dd}^{i,j} |\psi_j\rangle = \frac{C_{dd}}{8\pi|j-i|^3} \Big(\sin(\theta_i) \langle\psi_j| \sin(\theta_j) |\psi_j\rangle - 2\cos(\theta_i) \langle\psi_j| \cos(\theta_j) |\psi_j\rangle \Big) \quad . \tag{2.17}$$

Here $|\psi_j\rangle$ is the wave-function of the dipole **j** in the ground state. Taking into the ground state ordering for the classical limit, we assume that:

$$\sin(\theta_j) \to \langle \sin(\theta_j) \rangle = 0 \quad \text{and} \quad \cos(\theta_j) \to \langle \cos(\theta_j) \rangle = \Delta \quad . \tag{2.18}$$

Using this potential felt for the dipole $i = 0$ in *eq.*(2.6) can be re-written as follows:

$$V_{dd} = -\frac{C_{dd}}{8\pi} \Delta \cos(\theta) \zeta(3) \quad . \tag{2.19}$$

Thus, the Hamiltonian for a single dipole can be written as follows:

$$\hat{H} = -\frac{\hbar^2}{2I} \frac{d^2}{d\theta^2} - D\Delta \cos(\theta) \quad , \tag{2.20}$$

where:

$$D = \frac{C_{dd}}{8\pi}\zeta(3) \tag{2.21}$$

Writing the Schrödinger equation, we will have:

$$-\frac{\hbar^2}{2I}\frac{d^2}{d\theta^2}\psi(\theta) - D\Delta\cos(\theta)\psi(\theta) = E\psi(\theta) \quad . \tag{2.22}$$

Introducing a new variable $\theta = 2\eta$, we can re-write our equation as follows:

$$-\frac{\hbar^2}{8I}\frac{d^2}{d\eta^2}\psi(\eta) - D\Delta\cos(2\eta)\psi(\eta) = E\psi(\eta) \quad . \tag{2.23}$$

Multiplying both sides of the eq.(2.23) by $-8I/\hbar^2$ and introducing the following notations:

$$\epsilon = \frac{8IE}{\hbar^2} \quad \text{and} \quad q = \frac{4ID}{\hbar^2}\Delta \quad , \tag{2.24}$$

we will have:

$$\frac{d^2}{d\eta^2}\psi(\eta) + \Big(\epsilon + 2q\cos(2\eta)\Big)\psi(\eta) = 0 \quad . \tag{2.25}$$

Before we continue lets look at the properties of the wavefunction. Let us shift the angle η by $\eta \to \eta + \pi$. Since $\cos(2\eta + 2\pi) = \cos(2\eta)$, we will have:

$$\psi(\eta + \pi) = \psi(\eta) \tag{2.26}$$

Since we know how the equation for our system looks like (see *eq.*(2.25)), we can start a head-on calculation of the equation. On the other hand one can notice that this equation is the same as the *Mathieu equation*. Hence, before we continue solving *eq.*(2.25), let us see the properties of the Mathieu equation.

2.3 Mathieu Equation, Mathieu Functions

In [5] and [6], *Mathieu equation* is written as follows (**20.1.1** in [5]):

$$\frac{d^2}{d\eta^2}\psi(\eta) + \Big(a - 2q\cos(2\eta)\Big)\psi(\eta) = 0 \tag{2.27}$$

Here a, $q > 0$ are constants and η runs from zero to π. It is easy to notice that the Mathieu equation itself has a periodicity of π: *eq.*(2.27) is invariant under the trivial shift of the variable η by angle π: $\psi(\eta + \pi) = \psi(\eta)$.

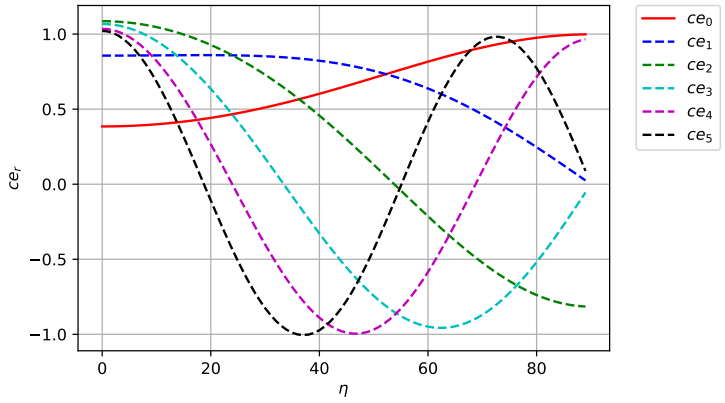

Figure 2.7: Angular dependence of the even Mathieu function $ce_m(\eta, q)$ for $m = \{0, 1, 2, 3, 4, 5\}$. During plotting these functions we assumed that $q = 1$.

In general, Mathieu equation has four series of distinct periodic solutions, two of them being even and two - odd. These solutions, generally called as *Mathieu functions*, are given as follows:

$$ce_{2m}(\eta, q) = \sum_{r=0}^{\infty} A_{2r}^{(2m)} \cos(2r\eta); \quad ce_{2m+1}(\eta, q) = \sum_{r=0}^{\infty} A_{2r}^{(2m+1)} \cos\big((2r+1)\eta\big) \quad , \tag{2.28}$$

$$se_{2m+1}(\eta, q) = \sum_{r=0}^{\infty} B_{2r}^{(2m+1)} \sin\big((2r+1)\eta\big); \quad se_{2m+2}(\eta, q) = \sum_{r=0}^{\infty} B_{2r}^{(2m+2)} \sin\big((2r+2)\eta\big) \quad . \tag{2.29}$$

Coefficients $A_{2r}^{(2m)}$, $A_{2r}^{(2m+1)}$ and $B_{2r}^{(2m+1)}$, $B_{2r}^{(2m+2)}$, also called the *Fourier* coefficients of the Mathieu functions, are functions of parameter **q**. In the *Figure* (2.7) we show the angular dependence of the even Mathieu function $ce_m(\eta, q)$ for $m = \{0, 1, 2, 3, 4, 5\}$. For each plots we assumed that $q = 1$. In general, solutions of the Mathieu equation are normalized such that:

$$\int_0^{2\pi} d\eta |\psi(\eta)|^2 = \pi \quad . \tag{2.30}$$

The eigenvalues of the above equation are usually denoted as follows: a_{2m}, a_{2m+1}, b_{2m}, b_{2m+1}. They are generally referred as the *characteristic values*. These characteristic values are the functions of **q**, and they are given in the forms of infinite series (see **20.2.25** in [5]). As an example, we give the formula for $\mathbf{a}_0$:

$$a_0(q) = -\frac{q^2}{2} + \frac{7q^4}{128} - \frac{29q^6}{2304} + \ldots \quad . \tag{2.31}$$

In the *Figure* (2.8) we have plotted the lowest energy eigenvalues $\mathbf{a}_0$, $\mathbf{a}_1$ and $\mathbf{b}_1$, $\mathbf{b}_2$ of the Mathieu equation. From the figure it is trivial to deduce that $\mathbf{a}_0$ is the lowest energy eigenvalue.

This eigenvalue corresponds to the even periodic Mathieu function $\boldsymbol{ce}_0$, which is represented as a continuous red line in *Figure* (2.7).

Before we continue with our equation, let us give one more property of the Mathieu functions. This property will be very useful in the following sections. If we make a following shift of the variable in eq.(2.27):

$$\eta \to \pm\big(\pi/2 \pm \eta\big) \quad , \tag{2.32}$$

we can re-write the Mathieu equation as follows (see **8.651** in [6]):

$$\frac{d^2}{d\eta^2}\psi(\eta) + \Big(a + 2q\cos(2\eta)\Big)\psi(\eta) = 0 \quad . \tag{2.33}$$

Then, Mathieu functions will transform accordingly:

$$ce_{2m}(\eta, q) = (-1)^m ce_{2m}\left(\frac{\pi}{2} - \eta, q\right); \quad ce_{2m+1}(\eta, q) = (-1)^m ce_{2m+1}\left(\frac{\pi}{2} - \eta, q\right) \quad , \tag{2.34}$$

and

$$se_{2m+1}(\eta, q) = (-1)^m se_{2m+1}\left(\frac{\pi}{2} - \eta, q\right); \quad se_{2m+2}(\eta, q) = (-1)^m se_{2m+2}\left(\frac{\pi}{2} - \eta, q\right). \tag{2.35}$$

Hence, we know that the *lowest energy eigenvalue* for the Mathieu equation (2.27) is $\mathbf{a}_0$ with wave-function $\boldsymbol{ce}_0(\eta, q)$. and from *eq.*(2.34) we know how the wave-functions are transformed (see *eq.*(2.33)).

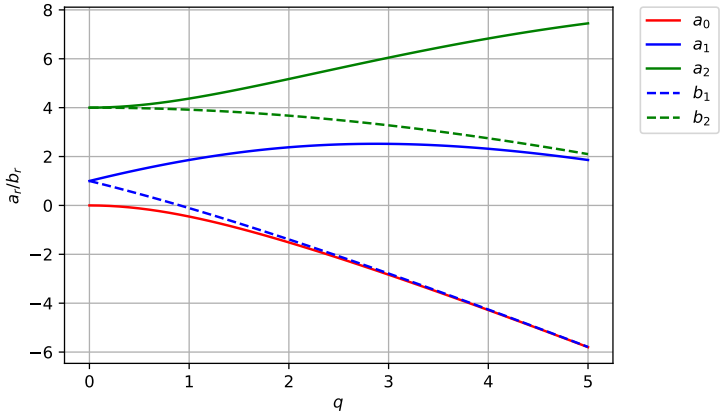

Figure 2.8: Four energy eigenvalues of the Mathieu equation (see eq.(2.27)). a_0 and a_1 are the eigenvalues for the eigenvector ce_0 and ce_q, whereas b_1

Thus, using the knowledge obtained for *Mathieu equation* and *Mathieu functions* we can continue solving the Schrödinger equation.

2.4 Weak Interaction Limit: $q << 1$

Knowing all necessary properties of the Mathieu equation, we can start solving our Schrödinger equation:

$$\frac{d^2}{d\eta^2}\psi(\eta) + \Big(\epsilon + 2q\cos(2\eta)\Big)\psi(\eta) = 0 \quad . \tag{2.36}$$

In order to observe the quantum phase transition, as we discussed earlier, we have to assume that $\mathbf{T} > \mathbf{V}$, where $\mathbf{T}$ represents the kinetic energy of a dipole and $\mathbf{V}$ - the mean-field potential. Mathematically this assumption is the same as assuming:

$$q << 1 \quad .$$

As it turns out, for $\mathbf{q}<< 1$ we can expand the ground state wave-function $\psi_0(\eta)$ of the system as a power series in $\mathbf{q}$. Including only terms up to the second order in $\mathbf{q}$, we can write:

$$\psi_0(\eta) = \frac{1}{\sqrt{\pi}} ce_0\Big(\frac{\pi}{2}\eta, q\Big) = \frac{1}{\sqrt{2\pi}}\Big(1 + \frac{q}{2}\cos(2\eta) + \frac{q^2}{32}\big(\cos(4\eta) - 2\big)\Big) \tag{2.37}$$

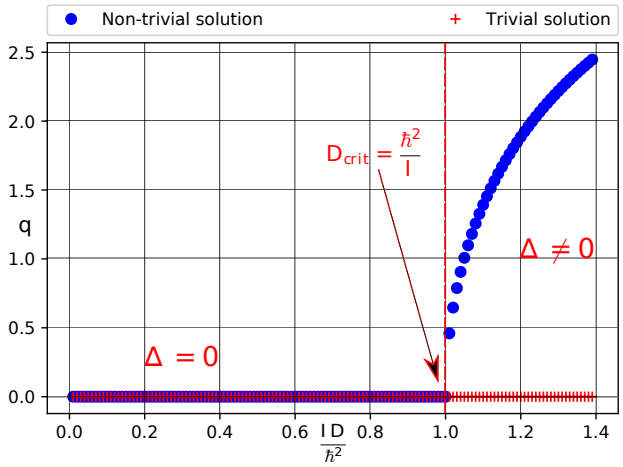

Figure 2.9: Trivial (red crosses) and non-trivial (blue balls) solutions for the self-consistent equation (2.41). We see that at $D = \hbar^2/I$ there is a phase transition from disordered phase to ordered phase.

In order to obtain the self-consistent equation, we have to calculate $\Delta = \langle\psi_0|\cos 2\eta\,|\psi_0\rangle$. We will have:

$$\begin{aligned}\langle\cos(2\eta)\rangle &= \frac{1}{2\pi}\int_0^\pi d\eta\cos(2\eta)\Big(1 + \frac{q}{2}\cos(2\eta) + \frac{q^2}{32}\big(\cos(4\eta) - 2\big)\Big)^2 \\ &= \frac{1}{2\pi}\int_0^\pi d\eta\cos(2\eta)\Big(1 + q\cos(2\eta) + \frac{q^2}{4}\cos^2(2\eta) + \frac{q^2}{16}\big(\cos(4\eta) - 2\big)\Big) \quad ,\end{aligned} \tag{2.38}$$

where we kept only the first and the second orders of $\mathbf{q}$. Doing the integration, we will obtain:

$$\langle\cos(2\eta)\rangle = \frac{q}{4}\Big(1 - \frac{3q^2}{64}\Big) \quad . \tag{2.39}$$

Now, remember that:

$$\Delta = \langle\cos(2\eta)\rangle = \frac{q\hbar^2}{4ID} \quad , \tag{2.40}$$

Thus, we will obtain:

$$q^3 = q\frac{64}{3}\left(1 - \frac{\hbar^2}{ID}\right) \quad . \tag{2.41}$$

Eq.(2.41) is the self-consistent equation for **q**. It is clear that this equation has both *trivial* and *non-trivial* solutions. The trivial solution is $q = 0$ for any value of **D**, where the non-trivial is:

$$q^2 = \frac{64}{3}\left(1 - \frac{\hbar^2}{ID}\right) \quad \Rightarrow \quad q = \pm 8\sqrt{\frac{1}{3}\left(1 - \frac{\hbar^2}{ID}\right)} \tag{2.42}$$

From the second equality in *eq.*(2.42) it is clear that when:

$$D < \frac{\hbar^2}{I} \quad , \tag{2.43}$$

q in *eq.*(2.42) becomes a complex number. Since we have a requirement that parameter **q** is real and positive, *eq.*(2.41) for $D < \hbar^2/I$ will only have the trivial solution:

$$q = 0 \quad \Rightarrow \quad \langle \cos(2\eta) \rangle = 0 \quad . \tag{2.44}$$

Before we continue let us stop here and discuss the obtained result. So far we have found that for $D < \hbar^2/I$ there exists a solution where $\langle \cos(2\eta) \rangle = 0$. This means that *all dipoles in the system on average have random orientation*. We will call this state a *highly disordered state*, pointing out that the orientation of one dipole is *not* affected by the orientation of another. Thus, one can argue that there exists a *local* (and also a global) $O(2)$ rotational symmetry in the system.

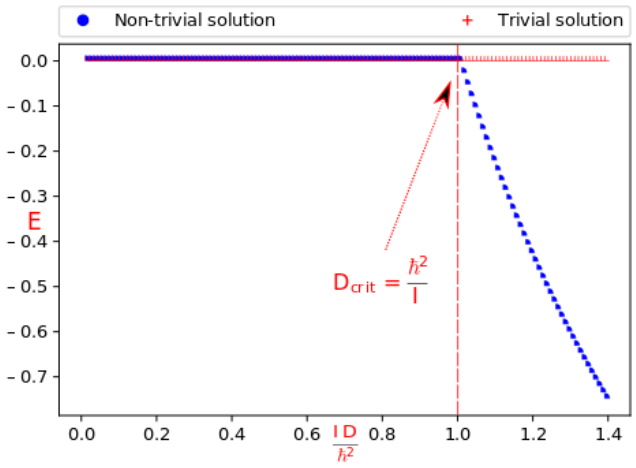

Figure 2.10: energy of the system as a function of $ID/\hbar^2$, for both trivial and non-trivial solution. We see that after the phase transition happens the non-trivial solution has the lowest energy, leading that for $D > D_{crit}$ the ground state is characterized with $\langle \cos(2\eta) \rangle \neq 0$.

Now, when $D > \hbar^2/I$, both trivial and non-trivial solutions exist (see *eq.*(2.42)). In order to see which of the solutions for $D > \hbar^2/I$ gives the *correct* behavior of the ground state of the system we have to calculate the energy of the system. From *eq.*(2.24) we know that:

$$E = \frac{\hbar^2 \epsilon}{8I} = \frac{\hbar^2 a_0}{8I} \quad , \tag{2.45}$$

where a_0 is given by eq.(2.31). Thus we will have:

$$E = -\frac{\hbar^2}{16I} q^2 \tag{2.46}$$

For *trivial* solution it is clear that $E = 0$ for any value of $\mathbf{D}$. For *non-trivial* solution we will have:

$$E = -\frac{4\hbar^2}{3I}\left(1 - \frac{\hbar^2}{ID}\right) \tag{2.47}$$

It is obvious from *eq.*(2.47) that the energy for the non-trivial solution has the lower value than for the trivial solution for $D > \hbar^2/I$. This can be seen in figure (2.10). With red crosses we have represented the energy of the system for trivial solutions, with blue balls - energy for non-trivial solution. We see that for $D < D_{crit}$ energies for both solutions coincide. Thus for $D < D_{crit}$ the system will choose the *highly disordered* state. After crossing the phase transition point:

$$D_{crit} = \frac{\hbar^2}{I} \quad , \tag{2.48}$$

which is two times the kinetic energy, we see that the system starts to order itself: $\Delta \neq 0$. We know from the classical limit (one can argue that in classical limit $D \to \infty$) dipoles are polarized along z-axis: $\Delta = 1$. For the sake of completeness and in order to see whether the MF approximation is correct, we will solve the Schrödinger equation for the limit when the potential energy of the system dominates over the kinetic energy. Mathematically this is the same as writing: $D \to \infty$.

2.5 Strong Interaction Limit: $D \to \infty$

Let us examine the strong interaction limit. As we mentioned earlier this is the limit when potential energy of the system dominates over the kinetic energy. First of all, let us re-write the initial Hamiltonian of the system:

$$\hat{H} = -\frac{\hbar^2}{2I}\frac{d^2}{d\eta^2} - D\Delta\cos(2\eta) \quad . \tag{2.49}$$

It is clear from the equation that the minimum of the potential is reached when $\eta = 0$. Hence, for large interaction limit, dipoles will *oscillate* around the potential minimum.

Taylor expanding the potential around its minimum and plugging into *eq.*(2.25), we will arrive at the following equation:

$$\frac{d^2}{d\eta^2}\psi(\eta) + \left(\epsilon^{'} - 4q\eta^2\right)\psi(\eta) = 0 \quad , \tag{2.50}$$

where $\epsilon^{'} = \epsilon + 2q$ is the rescaled energy. *Eq.*(2.50) has the same form as the equation for *harmonic oscillator*. It is obvious that the ground state wave-function for our system will be the ground state wave-function of the harmonic oscillator:

$$\psi_0(\eta) = \left(\frac{2\sqrt{q}}{\pi}\right)^{1/4} e^{-\sqrt{q}\eta^2} \quad . \tag{2.51}$$

Knowing this, it is trivial to calculate the value of Δ. We will have:

$$\langle 1 - 2\eta^2\rangle = 1 - 2\left(\frac{2\sqrt{q}}{\pi}\right)^{1/2}\int_0^{\pi} d\eta e^{-2\sqrt{q}\eta^2}\eta^2 = 1 - \left(\frac{2\sqrt{q}}{\pi}\right)^{1/2}\int_{-\pi}^{\pi} d\eta e^{-2\sqrt{q}\eta^2}\eta^2 \quad . \tag{2.52}$$

Since $D \to \infty$ (or it is the same as assuming that $q \to \infty$), the exponent in the integral in *eq.*(2.52) will decay rapidly before reaching its boundaries. Hence, we can change the integration limits to $\pm\infty$ and argue that the introduced *error* will be so infinitesimally small, that we can safely neglect it. Thus, the integral will become a Gaussian integral:

$$\int_{-\infty}^{+\infty} d\eta e^{-2\sqrt{q}\eta^2}\eta^2 = \sqrt{\frac{\pi}{32}}\frac{1}{q^{3/4}} \tag{2.53}$$

Plugging eq.(2.53) in eq.(2.52) we will obtain:

$$\langle 1 - 2\eta^2\rangle = 1 - \left(\frac{2\sqrt{q}}{\pi}\right)^{1/2}\sqrt{\frac{\pi}{32}}\frac{1}{q^{3/4}} = 1 - \frac{1}{4\sqrt{q}} \quad . \tag{2.54}$$

Since we are in the limit of $D \to \infty$ (or we can also say $q \to \infty$) the second term in *eq.*(2.54) will become zero, leading to:

$$\Delta = \langle 1 - 2\eta^2 \rangle = 1 \quad , \tag{2.55}$$

meaning that for the strong interaction limit on average all dipoles will have $\eta = 0$ orientation. Since this is the same result that we obtained from the classical limit, we can say that the mean field approximation used in the previous chapter is correct.

Let us make a short summary of our findings before moving on.

2.5.1 A Short Summary

Investigating the one-dimensional chain of identical dipoles interacting with each other via a long-range dipole-dipole interaction, we have obtained that in the classical limit the system prefers *polarized* orientation: all dipoles are polarized either along the z-axis or anti-parallel to it. Our

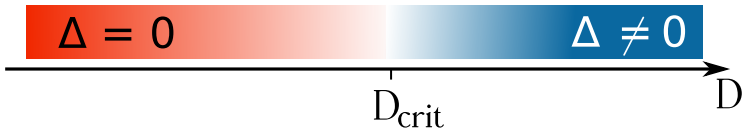

Figure 2.11: The phase diagram for the one-dimensional chain of identical dipoles interaction with each other via a long-range dipole-dipole interaction. For $D < D_{crit}$ we have *highly disordered* phase. $D = D_{crit}$ marks the quantum phase transition point. For $D > D_{crit}$ the system starts to order itself.

assumption, that the increase of the kinetic energy leads to the breaking of the ground state ordering, was correct. In the weak interaction limit ($\mathbf{T} > \mathbf{V}$) the system is in *highly disordered* phase. We also found the critical point $\mathbf{D}_{crit}$, where the quantum phase transition to *ordered* phase occurs.

In what follows, we give the explanation of the physics governing this system. Let us remember how the parameter $\mathbf{D}$ was introduced:

$$D = \frac{C_{dd}}{4\pi}\zeta(3), \quad \text{where} \quad C_{dd} = \frac{|d|^2}{\epsilon_0 a^3} \quad .$$

Here $|d|$ is the dipole moment (of water molecule) and $\epsilon_0 \approx 8.85 \times 10^{-12} Fm^{-1}$. Hence, a - being the distance between nearest neighbors - is the parameter that can be changed. Knowing this, the phase diagram represented in the *Figure* (2.11) can be explained in the following way: When identical dipoles are placed in the one-dimensional lattice such that the distance between nearest neighbors is: $a > a_{crit}$ (this corresponds to $D < D_{crit}$), the strength of the dipole-dipole interaction is weak, leading to the kinetic energy dominating over potential energy. This allows dipoles to have random orientation, thus $\Delta = 0$. If we now shrink our system, or place the dipoles close to each other such that $a < a_{crit}$ (this corresponds to $D > D_{crit}$) the strength od the dipole-dipole interaction becomes dominant over the kinetic energy and the dipoles begin to align themselves along (or anti-parallel) to z-axis.

The only question that is kept unanswered is: *what happens to the system of one-dimensional dipoles when the strength of the six-fold potential $U(\theta)$ is increased.* We will start dealing with this problem now.

2.6 Honeycomb Structure: A Tight-binding Model

In the previous sections we have always assumed that the potential created by the six membered ring of SiO_4 was so weak that its influence on the system could have been be neglected. This is why dipoles were able to rotate freely on any angle around y-axis. Now we make an opposite assumption. We assume that the potential created by this ring is strong. In the introduction, we have specified that the potential has the $\pi/3$ rotational symmetry, Hence, we can assume that the potential created by the honeycomb structure can ve written as a sum of six *Dirac-delta* functions:

$$V(\theta) = -\epsilon \sum_{m=1}^{6} \delta\left\{\frac{\pi}{3}(m-1) - \theta\right\} \quad . \tag{2.56}$$

We can thus argue, that the dipoles can arrange themselves at these following angles:

$$\theta_m = \left\{0; \frac{\pi}{3}; \frac{2\pi}{3}; \pi; \frac{4\pi}{3}; \frac{5\pi}{3}\right\} \quad . \tag{2.57}$$

In *eq.*(2.56) ϵ is the strength of the potential. The potential $U(\theta)$ is shown in the *Figure* (2.12). It is obvious that, since the dipole is constantly rotating inside the honeycomb structure, we have the periodic boundary condition.

Before we continue let us be sure that this potential has a $\pi/3$ rotational symmetry. Shifting $\theta \to \theta + \pi/3$, we will obtain:

$$V(\theta + \pi/3) = -\epsilon \sum_{m=1}^{6} \delta\left\{\frac{\pi}{3}(m-2) - \theta\right\} \quad . \tag{2.58}$$

Renaming the summation variable $m - 1 = \tilde{m}$, we will obtain:

$$V(\theta) = -\epsilon \sum_{\tilde{m}=1}^{6} \delta\left\{\frac{\pi}{3}(\tilde{m}-1) - \theta\right\} \quad , \tag{2.59}$$

which has the same form as the eq.(2.56), meaning that this potential truly has the $\pi/3$ rotational symmetry.

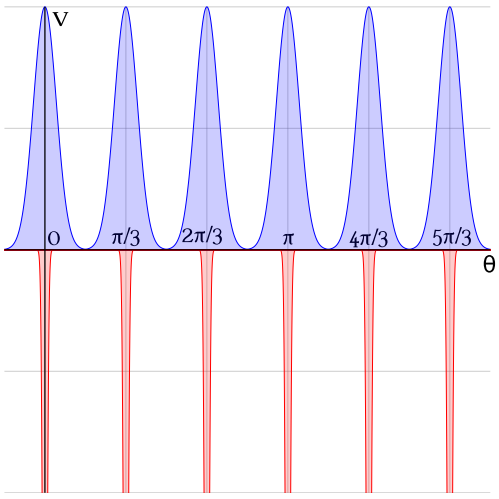

Figure 2.12: Wave-function of the test particle (Blue) and the delta function potential $U(\theta)$ (Red).

In order to see how the addition of the six-fold potential effects the system, let us make the following *thought experiment*. Let us place a *test particle* on the tip of the dipole moment vector.

This test particle can tunnel from one delta potential to another. Remembering that we have the periodic boundary condition, we can call each minimum of the potential a *lattice site* and picture the six-fold potential $U(\theta)$ as a one-dimensional lattice: in the *Figure* (2.12) we show a unit cell consisting of six lattice sites (six *delta* potentials). Hence, the rotation of the dipole moment can be described with the test particle hopping from one *lattice site* to another. We can argue that the wave-function of the test particle is strongly localized on any lattice site (see *Figure* (2.12)). Knowing all this, we can use the *tight-binding model* and write the Hamiltonian of the test particle in the second quantized form. For this we introduce the *angular* creation (annihilation) operators $\hat{c}_m^+$ ($\hat{c}_m$), which create (annihilate) the test particle on lattice cite **m** (**m+1**). It is clear that knowing the position of a test particle, we will also know at what angle (relative to quantization axis) is the dipole rotated.

The Hamiltonian for the test particle hopping from one site to another can be written as follows:

$$\hat{H} = -t \sum_{m=1}^{m=6} \left(c_m^\dagger c_{m+1} + h.c \right) \quad , \tag{2.60}$$

where **t** is the hopping amplitude of the test particle. Since we have the periodic boundary condition: $c_7 = c_1$, we can change the upper limit of the sum from $m = 6$ to $m = \infty$ and write the Hamiltonian in Fourier space to find the energy eigenvalues. The Fourier transform of the creation and annihilation operators can be written as follows:

$$c_m^\dagger = \frac{1}{\sqrt{2\pi}} \sum_k e^{ikm} c_k^\dagger \quad \text{and} \quad c_m = \frac{1}{\sqrt{2\pi}} \sum_k e^{-ikm} c_k \quad . \tag{2.61}$$

Plugging *eq.*(2.61) in *eq.*(2.60) we will obtain:

$$\begin{aligned} \hat{H} &= -\frac{t}{2\pi} \sum_m \sum_{k,\tilde{k}} e^{im(k-\tilde{k})} e^{-i\tilde{k}} c_k^\dagger c_{\tilde{k}} + h.c. \\ &= \sum_k E(k) c_k^\dagger c_k \quad , \end{aligned} \tag{2.62}$$

where $E(k) = -2t\cos(k)$ is the energy of the system. Here we have to remember, that even though we have treated the system as infinite, parameter k can takes only these *six* discrete values:

$$k_m = \left\{ 0; \frac{\pi}{3}; \frac{2\pi}{3}; \pi; \frac{4\pi}{3}; \frac{5\pi}{3} \right\} \quad . \tag{2.63}$$

Thus we will have the following values energies:

$$E(0) = -2t; \quad E(\pi/3) = -t; \quad E(2\pi/3) = t \quad ,$$

and

$$E(\pi) = 2t; \quad E(4\pi/3) = t; \quad E(5\pi/3) = -t \quad .$$

From the results obtained above it is clear that $E(\pi/3) = E(5\pi/3)$ and $E(2\pi/3) = E(4\pi/3)$. This is due to the $\pi/3$ symmetry that comes from the potential itself. Since we know how to describe the dipole centered in the six membered ring of SiO_0, it is time to introduce the mean-field in the system. In *eq.*(2.20) θ was a continuous variable. Because of the restrictions of the main potential, we also have to discretized the angle in mean-field potential. Thus we will have:

$$V_{dd}^{MF} = -D\Delta\cos(\theta_m) \quad , \tag{2.64}$$

which in the second quantized form can be written as:

$$V_{dd}^{MF} = -\sum_{m=1}^{6} \mu_m c_m^\dagger c_m \quad . \tag{2.65}$$

Here $\mu_m = -D\Delta\cos(\theta_m)$. In the following chapter we will use the perturbation theory approach to see how the phase diagram of the one-dimensional chain of dipoles is altered when the potential created by the ring of SiO_4 is increased such that the mean-field can be treated as a perturbation.

2.7 Perturbation Theory Approach

In the previous chapter we were able to write down the hopping and the mean-field potential term in the second quantized form. Combining eq.(2.60) and eq.(2.65) we can write the total Hamiltonian for the system:

$$\hat{H} = -t \sum_{m=1}^{6} \left(\hat{c}_m^\dagger \hat{c}_{m+1} + h.c \right) + \sum_{m=1}^{6} \mu_m \hat{c}_m^\dagger \hat{c}_m \quad . \tag{2.66}$$

Here we make the assumption: we assume that the strength of the mean-field is weak compared to the hopping term in eq.(2.66). thus we can treat the mean-field potential as a *perturbation* in the system. The wave-function of the unperturbed hopping Hamiltonian in eq.(2.66) can be written in the matrix form:

$$|k^0\rangle = \alpha_k \begin{pmatrix} e^{ik\theta_1} \\ e^{ik\theta_2} \\ e^{ik\theta_3} \\ e^{ik\theta_4} \\ e^{ik\theta_5} \\ e^{ik\theta_6} \end{pmatrix} \quad \text{where} \quad \alpha_k = \frac{1}{\sqrt{6}} \quad . \tag{2.67}$$

One can easily obtain that the wavefunction $|k^0\rangle$ is normalized:

$$\langle k^0 | k^0 \rangle = 1 \quad . \tag{2.68}$$

In general, when a perturbation is applied, the wave-functions and the energies of the total system are changed in the following manner:

$$|n\rangle = |n^0\rangle + q \sum_{k \neq n} \frac{\langle k^0 | V | n^0 \rangle}{E_n^0 - E_k^0} |k^0\rangle + q^2 \sum_{k \neq n} \sum_{l \neq n} \frac{\langle k^0 | V | l^0 \rangle \langle l^0 | V | n^0 \rangle}{(E_n^0 - E_k^0)(E_n^0 - E_l^0)} |k_0\rangle \quad , \tag{2.69}$$

and

$$\begin{aligned} E_n &= E_n^0 + q \langle n^0 | V | n^0 \rangle + q^2 \sum_{k \neq n} \frac{|\langle k^0 | V | n^0 \rangle|^2}{E_n^0 - E_k^0} \\ &\quad + q^3 \sum_{k \neq n} \sum_{l \neq n} \frac{\langle n^0 | V | l^0 \rangle \langle l^0 | V | k^0 \rangle \langle k^0 | V | n^0 \rangle}{(E_n^0 - E_k^0)(E_n^0 - E_l^0)} \\ &\quad - q^3 \langle n^0 | V | n^0 \rangle \sum_{l \neq n} \frac{|\langle n^0 | V | l^0 \rangle|^2}{E_n^0 - E_l^0} \quad , \end{aligned} \tag{2.70}$$

where $V = -\cos(\theta_m)$ and $E_k^0 = -2t\cos(k)$. Without any loss of generality we can write:

$$\begin{aligned} E &= \langle \psi(\theta) | \hat{H}_0 | \psi(\theta) \rangle + q \langle \psi(\theta) | V(\theta) | \psi(\theta) \rangle \\ &= \langle \psi(\theta) | \hat{H}_0 | \psi(\theta) \rangle - q \langle \psi(\theta) | \cos(\theta_m) | \psi(\theta) \rangle \end{aligned} \tag{2.71}$$

Since the unperturbed hopping Hamiltonian does not depend on $\mathbf{q}$, we can write the following:

$$\frac{dE}{dq} = -\langle \psi(\theta) | \cos(\theta_m) | \psi(\theta) \rangle = -\langle \cos(\theta_m) \rangle \tag{2.72}$$

Before continuing our calculations, let us calculate the following:

$$\begin{aligned}\langle k^0|\cos(\theta_m)\,|\tilde{k}^0\rangle &= \frac{1}{6}\begin{pmatrix} e^{ik\theta_1}\\ e^{ik\theta_2}\\ e^{ik\theta_3}\\ e^{ik\theta_4}\\ e^{ik\theta_5}\\ e^{ik\theta_6}\end{pmatrix}^{\dagger}\begin{pmatrix}\cos\theta_1 & 0 & 0 & 0 & 0 & 0\\ 0 & \cos\theta_2 & 0 & 0 & 0 & 0\\ 0 & 0 & \cos\theta_3 & 0 & 0 & 0\\ 0 & 0 & 0 & \cos\theta_4 & 0 & 0\\ 0 & 0 & 0 & 0 & \cos\theta_5 & 0\\ 0 & 0 & 0 & 0 & 0 & \cos\theta_6\end{pmatrix}\begin{pmatrix} e^{i\tilde{k}\theta_1}\\ e^{i\tilde{k}\theta_2}\\ e^{i\tilde{k}\theta_3}\\ e^{i\tilde{k}\theta_4}\\ e^{i\tilde{k}\theta_5}\\ e^{i\tilde{k}\theta_6}\end{pmatrix}\\ &= \frac{1}{6}\sum_{m=1}^{m=6} e^{i\theta_m\left(\tilde{k}-k\right)}\cos\theta_m \end{aligned} \tag{2.73}$$

Using the *eq.*(2.73) we will obtain the following:

$$\langle 0^0|\cos(\theta_m)\,|0^0\rangle = \frac{1}{6}\sum_{m=1}^{m=6}\cos\left\{\frac{m-1}{3}\pi\right\} = 0 \tag{2.74}$$

With this, it is clear to see that the second and the last terms of the *eq.*(2.70) will give zero. Hence, we can write:

$$E_n = E_n^0 + q^2\sum_{k\neq n}\frac{|\langle k^0|\,V\,|n^0\rangle\,|^2}{E_n^0 - E_k^0} + O(q^3) \tag{2.75}$$

The ground state of the Hamiltonian in *eq.*(2.66) will have the following shift:

$$E_0 = E_0^0 - \frac{q^2}{2t}\sum_{k\neq n}\frac{|\langle k^0|\,V\,|0^0\rangle\,|^2}{1-\cos(k)} + O(q^3) \tag{2.76}$$

Doing a derivative over $\mathbf{q}$ on the both sides of *eq.*(2.75), we will obtain:

$$\frac{dE_0}{dq} = -\frac{q}{t}\sum_{k\neq n}\frac{|\langle k^0|\,V\,|0^0\rangle\,|^2}{1-\cos(k)} + O(q^2) \tag{2.77}$$

Combining *eq.*(2.72) and *eq.*(2.77), we will obtain:

$$\langle\cos(\theta_m)\rangle = \frac{q}{t}\sum_{k\neq n}\frac{|\langle k^0|\,V\,|0^0\rangle\,|^2}{1-\cos(k)} + O(q^2) \tag{2.78}$$

It is clear to see that one can obtain the same *eq.*(2.78) starting from the new wavefunctions $|n\rangle$. It will go as follows:

$$|0\rangle = |0^0\rangle + \frac{q}{2t}\sum_{k\neq 0}\frac{\langle k^0|\cos(\theta_m)\,|0^0\rangle}{1-\cos(k)}\,|k^0\rangle + O(q^2) \quad .$$

Using this we can write:

$$\begin{aligned}\langle 0|\cos(\theta_m)\,|0\rangle &= \left\{\langle 0^0| + \frac{q}{2t}\sum_{k\neq 0}\frac{\langle 0^0|\cos(\theta_m)\,|k^0\rangle}{1-\cos(k)}\,\langle k^0| + O(q^2)\right\}\\ &\quad\times\cos(\theta_m)\left\{|0^0\rangle + \frac{q}{2t}\sum_{\tilde{k}\neq 0}\frac{\langle\tilde{k}^0|\cos(\theta_m)\,|0^0\rangle}{1-\cos(\tilde{k})}\,|\tilde{k}^0\rangle + O(q^2)\right\}\\ &= \langle 0^0|\cos(\theta_m)\,|0^0\rangle + \frac{q}{2t}\sum_{\tilde{k}\neq 0}\frac{\langle\tilde{k}^0|\cos(\theta_m)\,|0^0\rangle}{1-\cos(\tilde{k})}\,\langle 0^0|\cos(\theta_m)\,|\tilde{k}^0\rangle\\ &\quad + \frac{q}{2t}\sum_{k\neq 0}\frac{\langle 0^0|\cos(\theta_m)\,|k^0\rangle}{1-\cos(k)}\,\langle k^0|\cos(\theta_m)\,|0^0\rangle + O(q^2) \quad .\end{aligned}$$

Since $\langle 0^0|\cos(\theta_m)|0^0\rangle = 0$, we can write:

$$\begin{aligned}\langle 0|\cos(\theta_m)|0\rangle &= \frac{q}{2t}\sum_{\tilde{k}\neq 0}\frac{|\langle \tilde{k}^0|\cos(\theta_m)|0^0\rangle|^2}{1-\cos(\tilde{k})} + \frac{q}{2t}\sum_{k\neq 0}\frac{|\langle 0^0|\cos(\theta_m)|k^0\rangle|^2}{1-\cos(k)} + O(q^2)\\ &= \frac{q}{t}\sum_{k\neq 0}\frac{|\langle 0^0|\cos(\theta_m)|k^0\rangle|^2}{1-\cos(k)} + O(q^2) \quad ,\end{aligned}$$

which is the same equation as *eq.*(2.78).

We now have to remember that:

$$q = \frac{4ID}{\hbar^2}\Delta = \frac{4ID}{\hbar^2}\langle\cos(\theta_m)\rangle \tag{2.79}$$

Thus we will have:

$$\frac{\hbar^2 q}{4ID} = \frac{q}{t}\sum_{k\neq n}\frac{|\langle k^0|V|0^0\rangle|^2}{1-\cos(k)} \tag{2.80}$$

Bringing the following notation:

$$\delta = \sum_{k\neq n}\frac{|\langle k^0|V|0^0\rangle|^2}{1-\cos(k)} \tag{2.81}$$

we will have:

$$q\left(\frac{\hbar^2}{4ID} - \frac{\delta}{t}\right) = 0 \tag{2.82}$$

From the *eq.*(2.82) we can deduce that either $q = 0$ or:

$$D_{crit} = \frac{\hbar^2}{I}\frac{t}{4\delta} \tag{2.83}$$

Calculation of the numerical value for δ can be done using *eq.*(2.73) assuming that $|\tilde{k}\rangle = |0^0\rangle$. Hence, finally we will obtain:

$$D_{crit}^{new} = \frac{\hbar^2}{I}\frac{t}{4\delta} \quad . \tag{2.84}$$

Hence, we can observe that the critical point for quantum phase transition is changed and is depended on the value of hopping parameter **t**. Thus, the dipoles in the nano-cavities show a slightly different behavior. First of all, we can say that they are bound by the six-fold potential of the SiO_4: the potential $U(\theta)$ restricts them to have only six rotational orientations. When the mean-field is strong all dipoles are still polarized along or anti-parallel to z-axis. The most noticeable is the shift of the critical point: the new critical value for D is *larger* than for the system without the six-fold potential (assuming that $t > 4\delta$). This is due to the strength of the six-fold potential $U(\theta)$. Since it is a delta potential we have to give a test particle more energy (than it was needed for the system without this potential), which translates to increasing the strength of the dipole dipole interaction, in order to make it tunnel from, for example $k = \pi/3$ to $k = 0$.

In the next chapter we will start the investigation of two-dimensional systems.

Chapter 3

Two-dimensional systems of polar molecules

As the dimensionality of the system increases calculations become more and more complicated. This complication is due to the long range nature of the dipole-dipole interaction:

$$V \propto \frac{1}{r^3} \quad ,$$

where r is the distance between two interacting dipoles: during the calculations we have to take into account large number of dipoles. In the coarse of our research we were able to deduce that the intuition that we had for the one-dimensional chain was completely impractical for two and three dimension. Thus we have to do a more rigorous calculations in order to obtain the properties of the system.

In this chapter we will deal with the two-dimensional systems of polar molecules and investigate their phase diagrams.

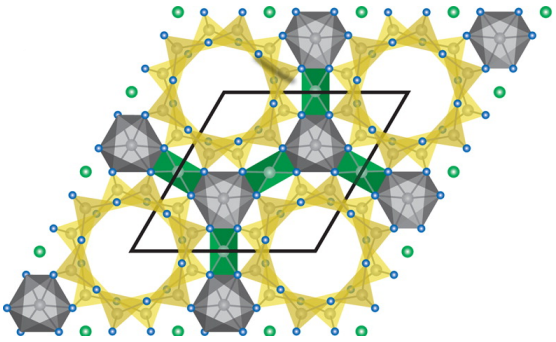

Figure 3.1: The Crystal structure of beryl in the plane perpendicular of the crystallographic c-axis [2]. the yellow triangles represent the SiO_4 molecules. The blue dots are oxygen atoms. The water molecules embedded in the system form a triangular lattice

First and foremost, we will discuss a *toy model*: the *quadratic lattice* of dipoles. In the beginning, as we did for the one-dimensional system, we will investigate the classical (strong interaction) limit. Choosing three different orderings: *polarized* (3.1.1), *striped* (3.1.2) and *checkerboard* (3.1.3), we will calculate the energy per particle and comparing with each other we will find the lowest energy solution. In order to find the quantum phase transition point we will write the Schrödinger equation using the mean-field approximation. Knowing the phase diagram we will add a six-fold potential to our system to calculate the shift of the critical point.

As depicted in the *Figure* (3.1), water molecules embedded in the beryl crystal form a triangular lattice. Initially we will assume that that the lattice is *ideal* (every lattice site is occupied with a

single water molecule). We will examine two different combinations appearing in triangular lattice. These are: *polarized* (3.2.1), and *striped* (3.2.2). Writing down the dipole-dipole interaction and comparing the potential energies (per particle) for these two configurations, we will be able to find the *ground state* configuration. Knowing this, we will write the mean-field potential and derive the Schröringer equation. Obtaining the self-consistent equation we will be able to find the critical point, where the quantum phase transitions occurs. We will also find that the ground state of dipoles in triangular lattice has a *global* $O(2)$ rotational symmetry.

During the research we asked ourselves: what would happen to the system (either globally or locally) if the lattice was not ideal, meaning there could exist defects or *deficiencies* in the system. In order to observe the changes of the symmetry of the system in the ground state we will will remove a single dipole from the lattice (3.3). Letting the system relax to a *local* ground state we observe how the local symmetry is disturbed.

3.1 Quadratic Lattice of Dipoles

Let us arrange **N** dipoles, interacting with each-other via a long-range dipole-dipole interaction, to form a quadratic lattice. We remind the reader, that during the calculations we will assume that our system is in thermodynamic limit, meaning that the results obtained will be the bulk properties of the system. In the *Figure* (3.2) we show such a system. Two unit vectors $\hat{a}_1$ and $\hat{a}_2$, being perpendicular to each other, span the whole two-dimensional surface. Moving along the x-axis we change the value of **i** and moving along y axis we change the value of **j**. We assume that the distance between two neighboring dipoles is $r_{i,j/i\pm1,j\pm1} = a$.

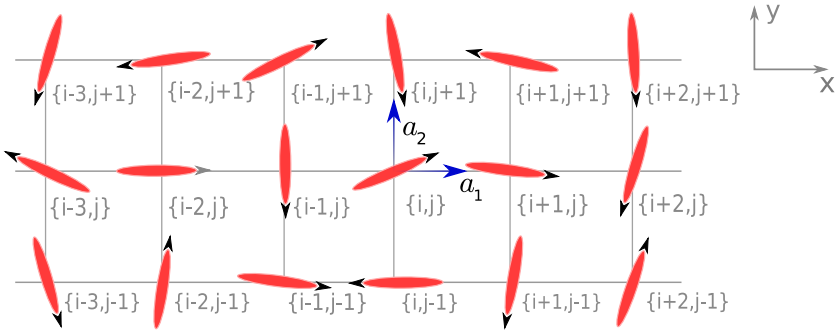

Figure 3.2: Quadratic lattice of identical dipoles. $\hat{a}_1$ and $\hat{a}_2$ are unit vectors connecting every lattice site to each other. We denote dipoles by "i, j", where i changes when we move along x-axis and j changes when we move along y-axis. The distance between two neighboring dipoles is equal to $r_{i,j/i\pm1,j\pm1} = a$.

The distance between two dipoles **i,j** and **i+m,j+n**, in general, can be written as follows:

$$\vec{r}_{i,j/i+m,j+n} = a\big(m\hat{a}_1 + n\hat{a}_2\big) \quad , \tag{3.1}$$

where

$$r^x_{i,j/i+m,j+n} = am \quad \text{and} \quad r^y_{i,j/i+m,j+n} = an \quad . \tag{3.2}$$

The general form of the dipole-dipole interaction between these two dipoles can be written as follows:

$$\begin{aligned} V_{dd}^{i,j/i+m,j+n} \quad &= \frac{1}{4\pi\epsilon_0|\vec{r}_{i,j/i+m,j+n}|^3}\Bigg(\vec{d}_{i,j}\cdot\vec{d}_{i+m,j+m} \\ &-3\frac{\big(\vec{r}_{i,j/i+m,j+n}\cdot\vec{d}_{i,j}\big)\big(\vec{r}_{i,j/i+m,j+n}\cdot\vec{d}_{i+m,j+n}\big)}{|\vec{r}_{i,j/i+m,j+n}|^2}\Bigg) \quad . \end{aligned} \tag{3.3}$$

As done in the one-dimensional case, we will write the potential using the spherical coordinates. We make the following restriction: dipoles are able to rotate in the surface of the lattice. For the first scalar product we will have:

$$\vec{d}_{i,j}\cdot\vec{d}_{i+m,j+n} = |d|^2\cos\Big(\theta_{i,j} - \theta_{i+m,j+n}\Big) \quad , \tag{3.4}$$

where $\theta_{i,j}$ is the angle between x-axis and the dipole moment $\vec{d}_{i,j}$ (see *Figure* (3.2)). For the second scalar product, appearing in the second part of the *eq.*(3.3), we will have:

$$\vec{r}_{i,j/i+m,j+n}\cdot\vec{d}_{i,j} = a|d|\Big(m\cos(\theta_{i,j}) + n\sin(\theta_{i,j})\Big) \quad . \tag{3.5}$$

Plugging *eq.*(3.4) and *eq.*(3.4) in V_{dd}, we will obtain:

$$\begin{aligned} V_{dd}^{i,j/i+m,j+n} &= \frac{|d|^2}{4\pi\epsilon_0 a^2\big(m^2+n^2\big)^{3/2}}\Bigg\{\cos(\theta_{i,j})\cos(\theta_{i+m,j+n})\bigg(1-\frac{3m^2}{m^2+n^2}\bigg) \\ &+\sin(\theta_{i,j})\sin(\theta_{i+m,j+n})\bigg(1-\frac{3n^2}{m^2+n^2}\bigg) \\ &-\frac{3mn}{m^2+n^2}\bigg(\sin(\theta_{i,j})\cos(\theta_{i+m,j+n})+\cos(\theta_{i,j})\sin(\theta_{i+,j+n})\bigg)\Bigg\} \quad , \end{aligned} \tag{3.6}$$

or by simplifying the form of the potential:

$$\begin{aligned} V_{dd}^{i,j/i+m,j+n} &= \frac{-|d|^2}{4\pi\epsilon_0 a^3\big(m^2+n^2\big)^{5/2}}\Big\{\big(2m^2-n^2\big)\cos(\theta_{i,j})\cos(\theta_{i+m,j+n}) \\ &+\big(2n^2-m^2\big)\sin(\theta_{i,j})\sin(\theta_{i+m,j+n}) \\ &+3mn\bigg(\sin(\theta_{i,j})\cos(\theta_{i+m,j+n})+\cos(\theta_{i,j})\sin(\theta_{i+,j+n})\bigg)\Big\} \quad . \end{aligned} \tag{3.7}$$

It is clear from the *eq.*(3.7), that potential has a $\pi/2$ rotational symmetry. Making the following shift of the angle $\theta \to \theta+\pi/2$ (also considering, that for this transformation $\mathbf{m}\to\mathbf{n}$ and $\mathbf{n}\to$ -$\mathbf{m}$), our potential will be invariant:

$$V_{dd}^{i,j/i+m,j+n}(\theta) = V_{dd}^{i,j/i+m,j+n}\bigg(\theta+\frac{\pi}{2}\bigg) \quad .$$

This is also expected due to the geometry of the lattice.

The potential energy of the dipole **i,j** due to interactions with all other **N-1** dipoles can be obtained by summing *eq.*(3.7) with **m** and **n**:

$$\begin{aligned} V_{dd}^{i,j} &= -\frac{C_{dd}}{4\pi}{\sum_{m,n}}'\frac{1}{\big(m^2+n^2\big)^{5/2}}\Big\{\big(2m^2-n^2\big)\cos(\theta_{i,j})\cos(\theta_{i+m,j+n}) \\ &+\big(2n^2-m^2\big)\sin(\theta_{i,j})\sin(\theta_{i+m,j+n}) \\ &+3mn\bigg(\sin(\theta_{i,j})\cos(\theta_{i+m,j+n})+\cos(\theta_{i,j})\sin(\theta_{i+,j+n})\bigg)\Big\} \quad , \end{aligned} \tag{3.8}$$

In the summation we have excluded the self-interaction term $\mathbf{m}=\mathbf{n}=0$ (we remind the reader that the summation for both **m** and **n** foes from $-\infty$ to ∞). Having in our hands the *classical* form of the dipole-dipole interaction potential, we can start calculating it for different configurations. One can argue that there exists numerous configurations for such a system. Since we want to find the lowest energy solution of the system, we will investigate three different configurations that have the potential to have the *lowest* energy. These configurations are: *polarized*, *striped* and *checkerboard* configuration. We will start with the 'textitpolarized configuration.

3.1.1 Polarized Configuration

Let us assume that the dipoles arranged in the square lattice are polarized at some angle ϕ (see *Figure* (3.3)). Thus, for our potential in *eq.*(3.8), for any value of $\mathbf{m}$ and $\mathbf{n}$, including $\mathbf{m} = \mathbf{n} = 0$,

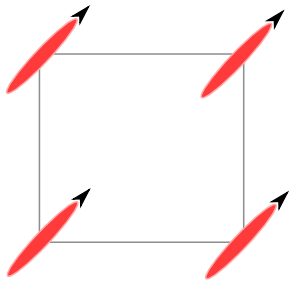

Figure 3.3: Unit cell of the quadratic lattice. The dipoles are in *polarized* configuration: $\theta_{i+m,j+n} = \phi$ for any value of $\mathbf{m}$ and $\mathbf{n}$, including $m = n = 0$.

we have to write:

$$\theta_{i+m,j+n} = \phi \quad . \tag{3.9}$$

Hence, we will obtain, that:

$$\begin{aligned} V_{dd}^{Pol} &= -\frac{C_{dd}}{4\pi} {\sum_{m,n}}' \frac{1}{\left(m^2+n^2\right)^{5/2}} \Big\{ \left(2m^2-n^2\right)\cos^2(\phi) + \left(2n^2-m^2\right)\sin^2(\phi) \\ &\quad +3mn\sin(2\phi) \Big\} \quad . \end{aligned} \tag{3.10}$$

Now, remember that we are looking at the system which is in thermodynamic limit, meaning that $N \to \infty$. Then it is clear that we can call the dipole **i,j** (for which we are writing the classical potential V_{dd}^{Pol}) a *central dipole*. Of course in thermodynamic limit one can argue that every dipole can be considered as a central central dipole, but we call dipole **i,j** central dipole for the sake of simplicity of the calculations. This means that every other dipole in the system will have the exactly same property as the dipole *i,j*. Hence, it is clear that:

$${\sum_{m,n}}' \frac{mn}{\left(m^2+n^2\right)^{5/2}} = 0 \quad , \tag{3.11}$$

since here and in *eq.*(3.10) summation for $\mathbf{m}$ and $\mathbf{n}$ goes from $-\infty$ to $+\infty$. Using this, our potential for the polarized state can be simplified into:

$$\begin{aligned} V_{dd}^{Pol} &= -\frac{C_{dd}}{4\pi} {\sum_{m,n}}' \frac{1}{\left(m^2+n^2\right)^{5/2}} \Big\{ \left(2m^2-n^2\right)\cos^2(\phi) + \left(2n^2-m^2\right)\sin^2(\phi) \Big\} \\ &= -\frac{C_{dd}}{4\pi} {\sum_{m,n}}' \frac{m^2}{\left(m^2+n^2\right)^{5/2}} \quad . \end{aligned} \tag{3.12}$$

We see from *eq.*(3.12), that the angular dependence vanishes, meaning that for any infinitesimal shift of the angle ϕ of the dipole orientation, the potential V_{dd}^{Pol} felt by the dipole **i,j** will stay *invariant*. Thus, for the polarized configuration our system of dipoles has a *global* $O(2)$ rotational symmetry.

The *Figure* (3.4) shows the polarized potential V_{dd}^{Pol} as a function of number of dipoles along x-axis in the system N_m. Here choose $C_{dd}/4\pi a^3 = 1$. We see that for large number of dipoles in the system (For our calculation we assumed that $N = 10^4$) the value of the potential saturates at around:

$$v_{dd}^{Pol} = \frac{4\pi}{C_{dd}} V_{dd}^{Pol} \approx -2.241 \quad . \tag{3.13}$$

Let us now move to the striped configuration.

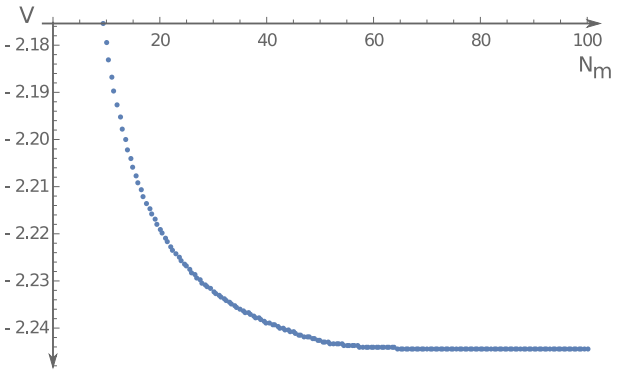

Figure 3.4: Potential V_{dd}^{Pol} (per particle) for the polarized configuration as a function of number of dipoles along x-axis: N_m. We have assumed that $C_{dd}/4\pi = 1$.

3.1.2 Striped Configuration

If the dipoles in the square lattice have striped configuration (*Figure* (3.5)), we can write:

$$\theta_{i+m,j+n} = \theta_{i,j} + n\pi \quad . \tag{3.14}$$

Thus:

$$\cos(\theta_{i+m,j+n}) = (-1)^n \cos(\theta_{i,j}) \quad \text{and} \quad \sin(\theta_{i+m,j+n}) = (-1)^n \sin(\theta_{i,j}) \quad . \tag{3.15}$$

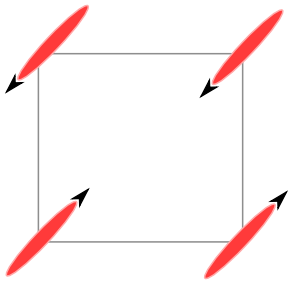

Figure 3.5: Unit cell of the quadratic lattice. The dipoles form the *striped* configuration: $\theta_{i+m,j+n} = \theta_{i,j} + n\pi$, for any value of $\mathbf{n}$, including $m = n = 0$.

Plugging *eq.*(3.15) in *eq.*(3.8) (and also making the following notation: $\theta_{i,j} = \phi$), we will obtain. that the potential for dipole **i,j** for striped configuration is:

$$V_{dd}^{Str} = -\frac{C_{dd}}{4\pi} {\sum_{m,n}}' \frac{(-1)^n}{\left(m^2+n^2\right)^{5/2}} \left(\left(2m^2 - n^2\right)\cos^2(\phi) + \left(2n^2 - m^2\right)\sin^2(\phi) \right) \tag{3.16}$$

Plotting the potential V_{dd}^{Str} as a function of ϕ revealed that angular dependence also vanishes (see *Figure* (3.6b)). Thus we again have a global $O(s)$ symmetry. Plotting V_{dd}^{Str} as a function of number of dipoles on x-axes N_m, we see, in the *Figure* (3.6a), that for large value of N_m ($N_m \approx 100$) the value starts to saturate.

We will obtain:

$$v_{dd}^{Str} = \frac{4\pi}{C_{dd}} V_{dd}^{Str} \approx -2.55 \quad . \tag{3.17}$$

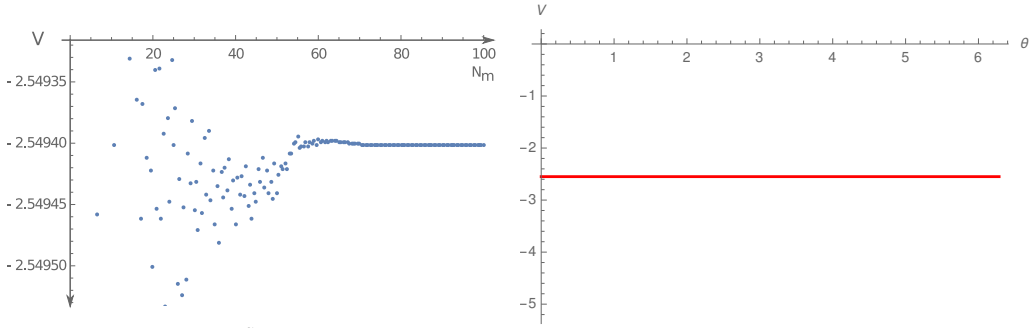

(a) $V_{dd}^{Str}(N_m)$ (b) $V_{dd}^{Str}(\phi)$

Figure 3.6: The potential V_{dd}^{Str} (per particle) of the striped configuration as a function N_m (a), and as a function of dipole orientation ϕ (b).

3.1.3 Checkerboard Configuration

For the checkerboard configuration (see *Figure* (3.7)), we assume that nearest neighbors have opposite orientation:

$$\theta_{i+m,j+n} = \theta_{i,j} + (m+n)\pi \quad . \tag{3.18}$$

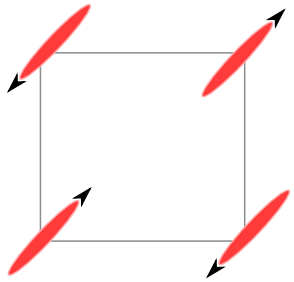

Figure 3.7: Unit cell of the quadratic lattice. The dipoles form a striped configuration: $\theta_{i+m,j+n} = \theta_{i,j} + (m+n)\pi$, for any value of $\mathbf{m}$ and $\mathbf{n}$, including $m = n = 0$.

Hence:

$$\cos(\theta_{i+m,j+n}) = (-1)^{m+n}\cos(\theta_{i,j}) \quad \text{and} \quad \sin(\theta_{i+m,j+n}) = (-1)^{m+n}\sin(\theta_{i,j}) \quad . \tag{3.19}$$

Plugging this in *eq.*(3.8), we will obtain:

$$V_{dd}^{Ch} = -\frac{C_{dd}}{4\pi a^3}{\sum_{m,n}}'(-1)^{m+n}\frac{m^2}{\left(m^2+n^2\right)^{5/2}} \quad , \tag{3.20}$$

where we see again that the angular dependence vanishes. Plotting V_{dd}^{Ch} as a function of N_m we obtain that for large number of dipoles along x-axis (for our calculations we assumed that the total number of dipoles was $N = 900$) the value of the potential saturates around a certain value (see *Figure* (3.8)):

$$v_{dd}^{Ch} = \frac{2\pi a^3}{C_{dd}}V_{dd}^{Ch} \approx -1.645 \quad . \tag{3.21}$$

3.1.4 The Mean-field Approximation

Let us look at the results that we have obtained: since the potential energy (per particle) for the striped orientation has the lowest value, we can say that in classical limit the system of dipoles

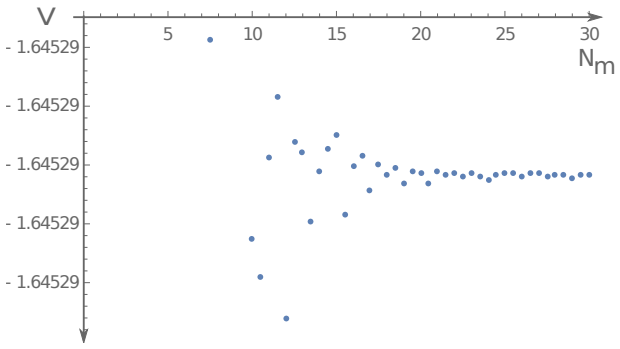

Figure 3.8: The potential V_{dd}^{Ch} (per particle) of the checkerboard configuration as a function N_m.

arranged in the quadratic lattice will choose the *striped* ordering in its ground state. *Before continuing our calculation, we want to mention that the analytical calculations done for classical limit are in perfect agreement with the results obtained in* [4] (see Figure (5) in [4])

Now, we let the kinetic energy of each dipole to increase. We can, of course, use the same argument that we used for one-dimensional system: the oscillations introduced by the kinetic energy will eventual become strong and will destroy the ground state ordering of the system. In order to observe this phenomenon and find the *phase transition* point, we will write the dipole-dipole interaction potential in the mean-field approximation. We will have:

$$\begin{aligned}
\langle\psi_{m,n}|\, V_{dd}^{i,j/i+m,j+n}\, |\psi_{m,n}\rangle &= -\frac{C_{dd}}{4\pi}{\sum_{m,n}}' \frac{1}{\left(m^2+n^2\right)^{5/2}} \\
&\times \Big\{ \left(2m^2-n^2\right)\cos(\theta_{i,j})\,\langle\psi_{m,n}|\cos(\theta_{i+m,j+n})\,|\psi_{m,n}\rangle \\
&+ \left(2n^2-m^2\right)\sin(\theta_{i,j})\,\langle\psi_{m,n}|\sin(\theta_{i+m,j+n})\,|\psi_{m,n}\rangle \\
&+ 3mn\Big(\sin(\theta_{i,j})\,\langle\psi_{m,n}|\cos(\theta_{i+m,j+n})\,|\psi_{m,n}\rangle \\
&+ \cos(\theta_{i,j})\,\langle\psi_{m,n}|\sin(\theta_{i+,j+n})\,|\psi_{m,n}\rangle \Big)\Big\} \quad . \qquad (3.22)
\end{aligned}$$

We remind the reader, that $C_{dd} = |d|^2/\epsilon_0 a^3$ and in the *classical* limit the system has the $O(2)$ rotational symmetry. Hence, the mean-field approximation can be written in the following way:

$$\begin{aligned}
\sin(\theta_{i+m,j+n}) \quad &\rightarrow \quad \langle\sin(\theta_{i+m,j+n})\rangle = 0 \quad \text{and} \\
&\cos(\theta_{i+m,j+n}) \rightarrow \langle\cos(\theta_{i+m,j+n})\rangle = (-1)^n\Delta \quad . \qquad (3.23)
\end{aligned}$$

Plugging *eq.*(3.23) into *eq.*(3.22), we will obtain:

$$\begin{aligned}
V_{dd}^{i,j} &= -\frac{C_{dd}\Delta}{4\pi}{\sum_{m,n}}' \frac{(-1)^n}{\left(m^2+n^2\right)^{5/2}}\Big\{\left(2m^2-n^2\right)\cos(\theta_{ij}) + 3mn\sin(\theta_{ij})\Big\} \\
&= -\frac{C_{dd}\Delta}{4\pi}{\sum_{m,n}}'(-1)^n \frac{\left(2m^2-n^2\right)}{\left(m^2+n^2\right)^{5/2}}\cos(\theta_{ij}) \quad . \qquad (3.24)
\end{aligned}$$

Here we've used the property that:

$${\sum_{m,n}}'(-1)^n \frac{mn}{\left(m^2+n^2\right)^{5/2}} = 0$$

We make a following notation:

$$C = {\sum_{m,n}}'(-1)^n \frac{\left(2m^2-n^2\right)}{\left(m^2+n^2\right)^{5/2}} \approx 2.94 \qquad (3.25)$$

Using this and eq.(3.24) the total Hamiltonian will become:

$$\hat{H} \quad = \quad -\frac{\hbar^2}{2I}\sum_{i,j}\frac{d^2}{d\theta_{ij}^2} - \frac{C_{dd}\Delta}{8\pi}\sum_{i,j} C\cos(\theta_{ij}) \quad . \tag{3.26}$$

Hence, using the mean-field approximation we were able to write the full Hamiltonian of the system as a sum of individual Hamiltonians describing single dipoles put in the mean field:

$$\hat{H}_{i,j} = -\frac{\hbar^2}{2I}\frac{d^2}{d\theta_{i,j}^2} - \frac{|d|^2\Delta}{8\pi\epsilon_0 a^3}C\cos(\theta_{i,j}) \quad . \tag{3.27}$$

In what follows we will omit the index **i,j**. The Schrödinger equation for single dipole put into a mean-field can be written:

$$-\frac{\hbar^2}{2I}\frac{d^2}{d\theta^2}\psi(\theta) - \frac{C_{dd}\Delta}{8\pi}C\cos(\theta)\psi(\theta) = E\psi(\theta) \quad , \tag{3.28}$$

which can also be written as:

$$\psi''(\theta) + \Big(\epsilon + 2q\cos(\theta)\Big)\psi(\theta) = 0 \quad , \tag{3.29}$$

where

$$\epsilon = -\frac{8I}{\hbar^2}E \quad \text{and} \quad q = \frac{4I}{\hbar^2}D\Delta, \quad \text{where} \quad D = \frac{C_{dd}}{8\pi}C \quad . \tag{3.30}$$

Eq.(3.29) for the quadratic lattice is the same as the *eq.*(2.25), which was derived for the one-dimensional chain of dipoles (see ***Chapter* 2**). The only difference between these two equations is the parameter - **D** - which is re-defined for the square lattice. Since the equation is the same, the critical value for the parameter **D**, where the phase transition occurs will be the same:

$$D_{crit} = \frac{\hbar^2}{I} \quad , \tag{3.31}$$

leading to:

$$C_{dd}^{crit} = \frac{8\pi}{IC}\hbar^2 \approx 8.5\frac{\hbar^2}{I} \tag{3.32}$$

When the kinetic energy dominates over the potential energy we know (from the observations done with one-dimensional chain), that system will be in highly disordered state: $\Delta = \langle\cos(\theta_{i+m,j+n})\rangle = 0$, and in the classical limit, when the potential energy is the dominant term, the system will have striped ordering.

3.1.5 A Short Summary

Within this *toy model*, we did the investigation of identical dipoles arranged into quadratic lattice. Calculating the dipole-dipole interaction (per particle), represented in *eq.*(3.8), we obtained that from three potential minimum energy configurations: polarized, striped and checkerboard the *striped* orientation, given by the following property:

$$\theta_{i+m,j+n} = \theta_{ij} + n\pi \quad ,$$

has the lowest energy.

Knowing the classical behavior of the system, we wrote the dipole-dipole potential in the mean-field approximation (see *eq.*(3.24)), and using it wrote the single-particle Schrödinger equation. It did turn out, that the equation for the square lattice is the same as for the one-dimensional chain, the only difference being that the parameter **D** in *eq.*(3.29) has to be redefined:

$$D = \frac{IC_{dd}}{8\pi\hbar^2}C \quad .$$

With this, we were able to find the critical value for **D** where the quantum phase transition from highly disordered $\Delta = 0$ to ordered $\Delta \neq 0$ phase occurs. Moreover, since the mean-field potential has the same form as for the one-dimensional chain, adding the six-fold potential will lead to the same results:

$$D^{'}_{crit} > D_{crit}$$

In the upcoming section we will start dealing with the lattice structure that is given in the experiment: we will arrange dipoles in the triangular lattice and investigate it's phase diagram.

3.2 Triangular Lattice of Dipoles

Let us assume that the dipoles (water molecules), which are interacting with each other via long-range dipole-dipole interaction form a triangular lattice. The figure (3.9) shows such kind of a system. In the figure $\hat{a}_1$ and $\hat{a}_2$ are unit vectors, connecting every lattice site to each other, such that:

$$\hat{a}_1 \cdot \hat{a}_2 = \cos(\theta_r) = \frac{1}{2} \quad .$$

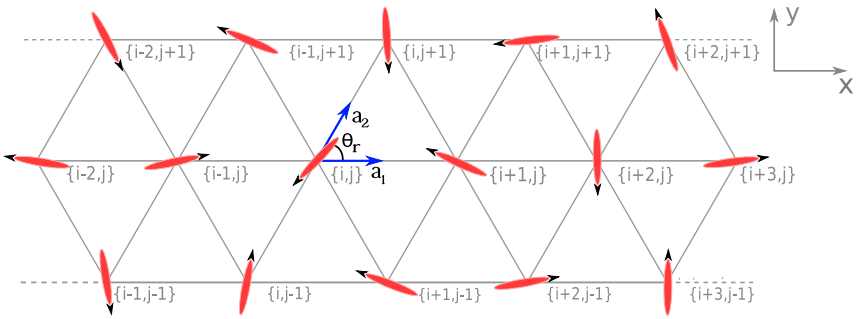

Figure 3.9: Triangular lattice of identical dipoles. $\hat{a}_1$ and $\hat{a}_2$ are unit vectors connecting every lattice site to each other. We denote dipoles by **i,j**, where **i** changes when we move along x-axis and **j** changes when we move along y-axis. Here $\theta_r = \pi/3$, and the distance between two neighboring dipoles is equal to $\boldsymbol{a}$.

As we did for the quadratic lattice, we call the dipole **i,j** *central* (remember that we again consider, that the system is in thermodynamic limit). Moving along the x-axis we change the value of the index **i**, and moving along y-axis the value of the index **j** is changed.

The distance between two dipoles **i,j** and **i+m,j+n** is given as follows:

$$\vec{r}_{i,j/i+m,j+n} = a\big(m\hat{a}_1 + n\hat{a}_2\big) \quad , \tag{3.33}$$

with:

$$r^x_{i,j/i+m,j+n} = a\left(m + \frac{n}{2}\right) \quad \text{and} \quad r^y_{i,j/i+m,j+n} = a\frac{n\sqrt{3}}{2} \quad . \tag{3.34}$$

Here $\boldsymbol{a}$ is the distance between two neighboring dipoles. In order to make derivations easier for the reader, we write the general form of the dipole-dipole interaction (between two dipoles **i,j** and **i+m,j+n**). We will have:

$$\begin{aligned} V_{dd}^{i,j/i+m,j+n} &= \frac{1}{4\pi\epsilon_0|\vec{r}_{i,j/i+m,j+n}|^3}\left(\vec{d}_{i,j}\cdot\vec{d}_{i+m,j+m}\right. \\ &\left. -3\frac{\left(\vec{r}_{i,j/i+m,j+n}\cdot\vec{d}_{i,j}\right)\left(\vec{r}_{i,j/i+m,j+n}\cdot\vec{d}_{i+m,j+n}\right)}{|\vec{r}_{i,j/i+m,j+n}|^2}\right) \quad . \end{aligned} \tag{3.35}$$

Writing the scalar product of two dipole moments in the first term of the *eq.*(3.35), we will have:

$$\vec{d}_{i,j}\cdot\vec{d}_{i+m,j+n} = |d|^2\cos\left(\theta_{i,j} - \theta_{i+m,j+n}\right) \quad , \tag{3.36}$$

where $\theta_{i,j}$ is the angle between x axis and the dipole moment $\vec{d}_{i,j}$ (see *Figure* (3.9)). We used the polar coordinate system to derive the scalar product in *eq.*(3.36) . For the scalar product between $\vec{r}_{i,j/i+m,j+n}$ and $\vec{d}_{i,j}$, appearing in the second term of the *eq.*(3.35), we will have:

$$\begin{aligned} \vec{r}_{i,j/i+m,j+n}\cdot\vec{d}_{i,j} &= r^x_{i,j/i+m,j+n}d^x_{i,j} + r^y_{i,j/i+m,j+n}d^y_{i,j} \\ &= a|d|\left\{\left(m+\frac{n}{2}\right)\cos(\theta_{i,j}) + \frac{n\sqrt{3}}{2}\sin(\theta_{i,j})\right\} \end{aligned} \tag{3.37}$$

Hence, we will have:

$$\begin{aligned}
&\big(\vec{r}_{i,j/i+m,j+n}\cdot\vec{d}_{i,j}\big)\big(\vec{r}_{i,j/i+m,j+n}\cdot\vec{d}_{i+m,j+n}\big)\\
&=a^2|d|^2\bigg(\bigg(m+\frac{n}{2}\bigg)\cos(\theta_{i,j})+\frac{n\sqrt{3}}{2}\sin(\theta_{i,j})\bigg)\\
&\times\bigg(\bigg(m+\frac{n}{2}\bigg)\cos(\theta_{i+m,j+n})+\frac{n\sqrt{3}}{2}\sin(\theta_{i+m,j+n})\bigg)\\
&=a^2|d|^2\bigg\{\cos(\theta_{i,j})\cos(\theta_{i+m,j+n})\bigg(m+\frac{n}{2}\bigg)^2+\sin(\theta_{i,j})\sin(\theta_{i+m,j+n})\frac{3n^2}{4}\\
&\frac{n\sqrt{3}}{2}\bigg(m+\frac{n}{2}\bigg)\bigg(\sin(\theta_{i,j})\cos(\theta_{i+m,j+n})+\cos(\theta_{i,j})\sin(\theta_{i+m,j+n})\bigg)\bigg\}
\end{aligned}\tag{3.38}$$

The only thing left, is to calculate $|\vec{r}_{i,j/i+m,j+n}|$. For this we can write:

$$|\vec{r}_{i,j/i+m,j+n}|^2=a^2\big(m\hat{a}_1+n\hat{a}_2\big)^2=a^2\big(m^2+n^2+mn\big)\tag{3.39}$$

Plugging *eq.*(3.36), *eq.*(3.38) and *eq.*(3.39) in *eq.*(3.35) for $V_{dd}^{i,j/i+m,j+n}$, we will find:

$$\begin{aligned}
V_{dd}^{i,j/i+m,j+n} &= \frac{C_{dd}}{4\pi|m^2+n^2+mn|^{3/2}}\bigg\{\cos(\theta_{i,j})\cos(\theta_{i+m,j+n})+\sin(\theta_{i,j})\sin(\theta_{i+m,j+n})\\
&-\frac{3}{|m^2+n^2+mn|}\bigg(\cos(\theta_{i,j})\cos(\theta_{i+m,j+n})\bigg(m+\frac{n}{2}\bigg)^2\bigg)\\
&+\sin(\theta_{i,j})\sin(\theta_{i+m,j+n})\frac{3n^2}{4}+\frac{n\sqrt{3}}{2}\bigg(m+\frac{n}{2}\bigg)\bigg(\cos(\theta_{i,j})\cos(\theta_{i+m,j+n})\\
&+\cos(\theta_{i,j})\sin(\theta_{i+m,j+n})\bigg)\bigg\}\quad .
\end{aligned}\tag{3.40}$$

Simplifying the potential in *eq.*(3.40), we will obtain:

$$\begin{aligned}
V_{dd}^{i,j/i+m,j+n} &= \frac{C_{dd}}{4\pi|m^2+n^2+mn|^{3/2}}\\
&\times\bigg\{\cos(\theta_{i,j})\cos(\theta_{i+m,j+n})\bigg(1-3\frac{\big(m+\frac{n}{2}\big)^2}{|m^2+n^2+mn|}\bigg)\\
&+\sin(\theta_{i,j})\sin(\theta_{i+m,j+n})\bigg(1-\frac{9}{4}\frac{n^2}{|m^2+n^2+mn|}\bigg)\\
&-\frac{3\sqrt{3}}{2}\frac{n\big(m+\frac{n}{2}\big)}{|m^2+n^2+mn|}\bigg(\sin(\theta_{i,j})\cos(\theta_{i+m,j+n})\\
&+\cos(\theta_{i,j})\sin(\theta_{i+m,j+n})\bigg)\bigg\}\quad .
\end{aligned}\tag{3.41}$$

The potential of dipole **i,j** due to the interactions with all **N−1** can be obtained by summing over all values of **m** and **n** except *m=n=0* (since we do not want to have self-interaction in our

potential). Thus we can write:

$$\begin{aligned} V_{dd}^{i,j} &= \sum_{m,n}{}' V_{dd}^{i,j/i+m,j+n} \\ &= \frac{C_{dd}}{4\pi} \sum_{m,n}{}' \frac{1}{|m^2+n^2+mn|^{3/2}} \\ &\left\{ \cos(\theta_{i,j})\cos(\theta_{i+m,j+n})\left(1-3\frac{\left(m+\frac{n}{2}\right)^2}{|m^2+n^2+mn|}\right)\right. \\ &+\sin(\theta_{i,j})\sin(\theta_{i+m,j+n})\left(1-\frac{9}{4}\frac{n^2}{|m^2+n^2+mn|}\right) \\ &\left.-\frac{3\sqrt{3}}{2}\frac{n\left(m+\frac{n}{2}\right)}{|m^2+n^2+mn|}\left(\sin(\theta_{i,j})\cos(\theta_{i+m,j+n})+\cos(\theta_{i,j})\sin(\theta_{i+m,j+n})\right)\right\} \quad ,(3.42) \end{aligned}$$

Using *eq.*(3.42) the total Hamiltonian of the system will be:

$$\begin{aligned} \hat{H} &= -\frac{\hbar^2}{2I}\sum_{i,j}\frac{d^2}{d\theta_{i,j}^2} + \frac{C_{dd}}{8\pi}\sum_{i,j}\sum_{m,n}{}' \frac{1}{|m^2+n^2+mn|^{3/2}} \\ &\left\{ \cos(\theta_{i,j})\cos(\theta_{i+m,j+n})\left(1-3\frac{\left(m+\frac{n}{2}\right)^2}{|m^2+n^2+mn|}\right)\right. \\ &+\sin(\theta_{i,j})\sin(\theta_{i+m,j+n})\left(1-\frac{9}{4}\frac{n^2}{|m^2+n^2+mn|}\right) \\ &\left.-\frac{3\sqrt{3}}{2}\frac{n\left(m+\frac{n}{2}\right)}{|m^2+n^2+mn|}\left(\sin(\theta_{i,j})\cos(\theta_{i+m,j+n})+\cos(\theta_{i,j})\sin(\theta_{i+m,j+n})\right)\right\} \quad (3.43) \end{aligned}$$

Let us first observe the *classical limit* for this system ($\mathbf{T} < \mathbf{V}$). There are numerous configurations that might exist in this system, but the two configurations: *polarized* and *striped* orderings, have a potential to be the *lowest energy configurations*. Thus, we have to do an in-depth calculation for each configuration in order to see which of these two configurations gives the lowest energy. For polarized configuration, as was introduced in quadratic lattice, we assume that all dipoles are oriented such that for any **i** and **j**:

$$\theta_{i,j} = \phi \tag{3.44}$$

For the striped orientation:

$$\text{if} \quad \theta_{i,j} = \phi \quad \text{then} \quad \theta_{i,j+n} = \phi + n\pi \quad . \tag{3.45}$$

Such configurations are shown in *Figure* (3.10). Let us start our calculations with the polarized configuration.

3.2.1 Polarized Configuration

Using *eq.*(3.44) in *eq.*(3.42), derived in previous section, we will obtain:

$$\begin{aligned} V_{dd}^{Pol} &= \frac{C_{dd}}{8\pi}\sum_{m,n}{}' \frac{1}{|m^2+n^2+mn|^{3/2}}\left\{ \cos^2(\phi)\left(1-3\frac{\left(m+\frac{n}{2}\right)^2}{|m^2+n^2+mn|}\right)\right. \\ &\left.+\sin^2(\phi)\left(1-\frac{9}{4}\frac{n^2}{|m^2+n^2+mn|}\right)-\frac{3\sqrt{3}}{2}\frac{n\left(m+\frac{n}{2}\right)}{|m^2+n^2+mn|}\sin(2\phi)\right\} \\ &= \frac{C_{dd}}{8\pi}\sum_{m,n}{}' \frac{1}{|m^2+n^2+mn|^{3/2}}\left\{1-\frac{3}{|m^2+n^2+mn|}\left(\cos^2(\phi)\left(m+\frac{n}{2}\right)^2\right.\right. \\ &\left.\left.+\frac{3n^2}{4}\sin^2(\phi)+n\frac{\sqrt{3}}{2}\left(m+\frac{n}{2}\right)\sin(2\phi)\right)\right\} \quad . \end{aligned} \tag{3.46}$$

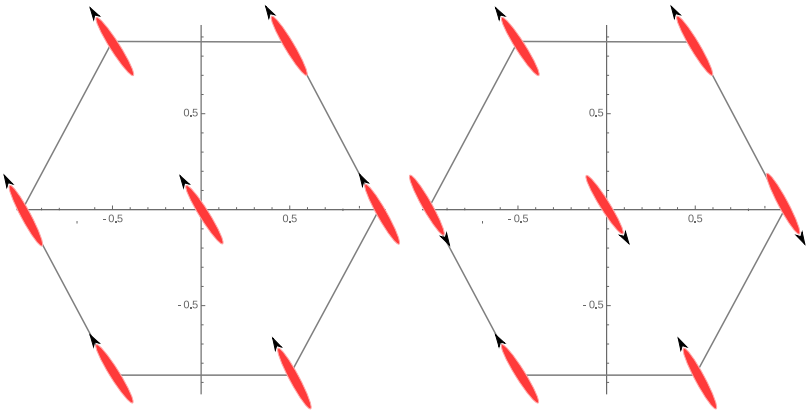

(a) Polarized (b) Striped

Figure 3.10: (a) Polarized configuration for the triangular lattice: $\theta_{i,j} = \phi$. (b) Striped orientation where, if $\theta_{i,j} = \phi$, $\theta_{i,j+n} = \phi + n\pi$.

Finally, after some simplifications, we will obtain:

$$V_{dd}^{Pol} = \frac{C_{dd}}{8\pi} {\sum_{m,n}}' \frac{1}{|m^2+n^2+mn|^{3/2}} \left\{ 1 - 3 \frac{\left(m\cos(\phi) + n\cos\left(\phi - \theta_r\right)\right)^2}{|m^2+n^2+mn|} \right\} \quad , \tag{3.47}$$

where, as mentioned in *Figure* (3.9), $\theta_r = \pi/3$. From *eq.*(3.47) it is clear that the potential has the following property.

Rotating every dipole by $\pi/3$ we will arrive:

$$\begin{aligned} V_{dd}^{Pol}\left(\phi + \frac{\pi}{3}\right) &= \frac{C_{dd}}{8\pi} {\sum_{m,n}}' \frac{1}{|m^2+n^2+mn|^{3/2}} \left\{ 1 \right. \\ &\quad \left. -3 \frac{\left(m\cos\left(\phi + \frac{\pi}{3}\right) + n\cos\left(\phi - \theta_r + \frac{\pi}{3}\right)\right)^2}{|m^2+n^2+mn|} \right\} \\ &= \frac{C_{dd}}{8\pi} {\sum_{m,n}}' \frac{1}{|m^2+n^2+mn|^{3/2}} \left\{ 1 \right. \\ &\quad \left. -3 \frac{\left(m\cos\left(\phi + \frac{\pi}{3}\right) + n\cos\left(\phi\right)\right)^2}{|m^2+n^2+mn|} \right\} \quad . \end{aligned}$$

Interchanging **m** with **n** (and vice versa) we will arrive at the same form of the potential as in *eq.*(3.47). This result is evident from the geometrical structure of the lattice: the lattice itself has a $\pi/3$ rotational symmetry.

We argue that there exists a *stronger* symmetry for system of the polarized dipoles in triangular lattice. Mainly, we will show here that such as system has an $O(2)$ rotational symmetry. In order to make it clear for the readers, we will do a following thought experiment. Let us introduce a cutoff radius $\mathbf{r}_{cut}$ such that if a dipole lies outside a circle of radius $\mathbf{r}_{cut}$, it's interaction with the dipole in the center of the circle can be neglected. Suppose that we make the cutoff radius such that the central dipole interacts only with its six nearest neighbors(see *Figure* (3.10a)). We will calculate the interaction between the central dipole and its neighbors and afterwards we will

increase the value of $\mathbf{r}_{cut}$, such that the thermodynamic limit will be preserved. If the central dipole is denoted as $\{i = 0, j = 0\}$, then the neighboring dipoles will be:

$$\{1,0\}; \quad \{-1,0\}; \quad \{0,1\}; \quad \{0,-1\}; \quad \{1,-1\}; \quad \{-1,1\} \quad .$$

From the symmetry of the honeycomb structure, it is obvious that:

$$V_{dd}^{1,0} = V_{dd}^{-1,0}; \quad V_{dd}^{0,1} = V_{dd}^{0,-1}; \quad V_{dd}^{1,-1} = V_{dd}^{-1,1} \quad . \tag{3.48}$$

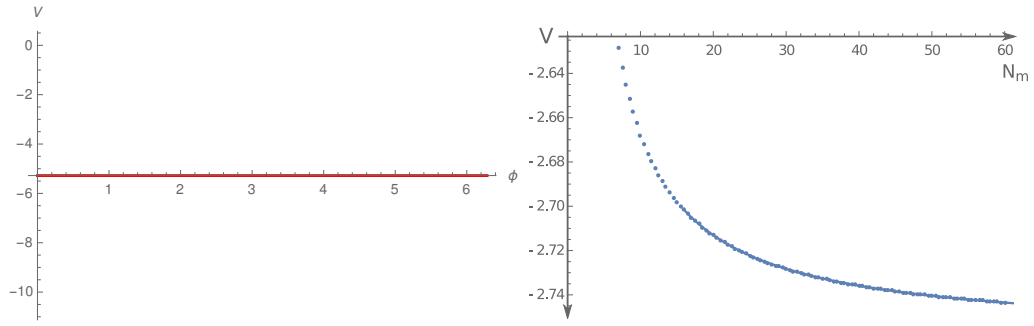

(a) $V_{dd}^{Pol}(\phi)$ (b) $V_{dd}^{Pol}(N)$

Figure 3.11: The total interaction V_{dd}^{Pol} (per one particle) for polarized configuration as a function of angle ϕ(a) and the total number of dipoles N(b) for the polarized configuration.

Using *eq.*(3.47), we can calculate the potential felt by the central dipole. We will obtain:

$$V_{dd}^{1,0} = \frac{C_{dd}}{8\pi}\Big(1 - 3\cos^2(\phi)\Big); \quad V_{dd}^{0,1} = \frac{C_{dd}}{8\pi}\left(1 - 3\sin^2\left(\phi + \frac{\pi}{6}\right)\right) \quad , \tag{3.49}$$

and

$$V_{dd}^{1,-1} = \frac{C_{dd}}{8\pi}\left\{1 - 3\Big(\cos(\phi) - \sin\left(\phi + \frac{\pi}{6}\right)\Big)^2\right\} \quad . \tag{3.50}$$

The total potential for dipole **i,j** will be the sum of there three interactions (multiplied by two):

$$\begin{aligned} V_{dd}^{total} &= 3\frac{C_{dd}}{4\pi}\left\{\sin^2(\phi) - \sin^2\left(\phi + \frac{\pi}{6}\right) - \left(\cos(\phi) - \sin\left(\phi + \frac{\pi}{6}\right)\right)^2\right\} \\ &= -3\frac{C_{dd}}{8\pi} \end{aligned} \tag{3.51}$$

From the *eq.*(3.51) we see that the angular dependence vanishes. We can now increase the cutoff radius $\mathbf{r}_{cut}$ such that more dipoles will appear inside the circle, meaning that the number of interacting dipoles $\mathbf{N}$ will increase. We observe that the overall value of V_{dd}^{Pol} in *eq.*(3.47) decreases as the value of $\mathbf{N}_m$, where $\mathbf{N}_m$ is the number of dipoles along x-axis, increases (see *Figure* (3.11b)). But the potential is always independent of the angle of polarization ϕ (see *Figure* (3.11a)). Notice that $N = N_m^2$. Hence, we can say that the polarized dipoles have the global $O(2)$ rotational symmetry. Assuming that dipoles are polarized at angle $\phi = \pi/2$, we can write the following final form of the dipole-dipole interaction:

$$\begin{aligned} V_d^{Pol} &= \frac{C_{dd}}{8\pi}{\sum_{m,n}}' \frac{1}{|m^2 + n^2 + mn|^{3/2}}\left(1 - \frac{3}{4}\frac{n^2}{|m^2 + n^2 + mn|}\right) \\ &\approx -2.72\frac{C_{dd}}{8\pi} \quad . \end{aligned} \tag{3.52}$$

Now let us move onto the striped orientation.

3.2.2 Striped Configuration

For the striped orientation, as shown in the *eq.*(3.45):

$$\cos(\theta_{i,j+n}) = (-1)^n \cos(\phi) \quad \text{and} \quad \sin(\theta_{i+m,j+n}) = (-1)^n \sin(\phi) \quad , \tag{3.53}$$

for any value of $\mathbf{n}$. Plugging this in *eq.*(3.42), we will obtain:

$$\begin{aligned} V_{dd}^{Str} &= \frac{C_{dd}}{8\pi} {\sum_{m,n}}' \frac{(-1)^n}{|m^2+n^2+mn|^{3/2}} \Bigg\{ \cos^2(\phi) \left(1 - 3\frac{\left(m+\frac{n}{2}\right)^2}{|m^2+n^2+mn|}\right) \\ &\quad + \sin^2(\phi)\left(1 - \frac{9}{4}\frac{n^2}{|m^2+n^2+mn|}\right) - \frac{3\sqrt{3}}{2}\frac{n\left(m+\frac{n}{2}\right)}{|m^2+n^2+mn|}\sin(2\phi)\Bigg\} \\ &= \frac{C_{dd}}{8\pi} {\sum_{m,n}}' \frac{(-1)^n}{|m^2+n^2+mn|^{3/2}} \left\{1 - 3\frac{\Big(m\cos(\phi) + n\cos\left(\phi-\theta_r\right)\Big)^2}{|m^2+n^2+mn|}\right\} \quad . \end{aligned} \tag{3.54}$$

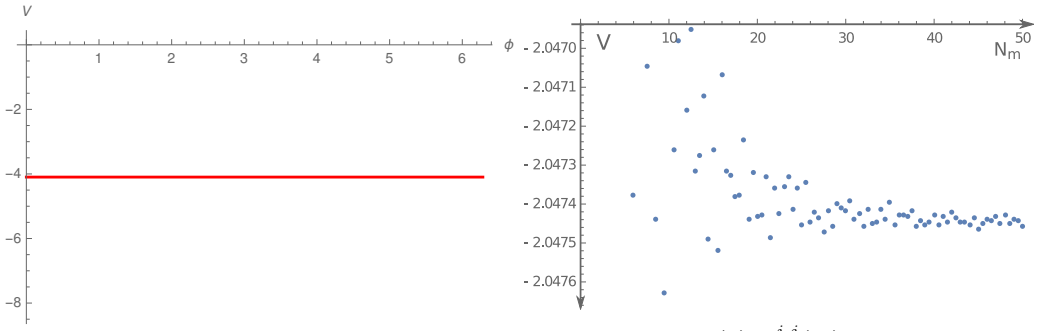

(a) $V_{dd}^{i,j}(\phi)$ (b) $V_{dd}^{i,j}(N)$

Figure 3.12: The total interaction per one particle V_{dd}^{Str} as a function of angle ϕ (a), and the total number of dipoles N (b) for the striped configuration.

Doing the same analysis that we did for the polarized configuration, we will obtain that V_{dd}^{Str} in *eq.*(3.54) also does not depend on angle ϕ (see the first plot of the figure (3.12)), meaning that again we have a global $O(2)$ rotational symmetry in the system. In the *Figure* (3.12a) we see the potential for striped configuration V_{dd}^{Str} as a function of total number of dipoles $\mathbf{N}_m$.

The potential V_{dd}^{Str} for $\phi = \pi/2$ will be as follows:

$$\begin{aligned} V_{dd}^{Str} &= \frac{C_{dd}}{8\pi} {\sum_{m,n}}' \frac{(-1)^n}{|m^2+n^2+mn|^{3/2}} \left\{1 - \frac{9}{4}\frac{n^2}{|m^2+n^2+mn|}\right\} \\ &\approx -2.05\frac{C_{dd}}{8\pi} \end{aligned} \tag{3.55}$$

From the second plots of figures (3.11) and (3.12) it is clear that the polarized orientation has the lowest energy. *Moreover, the analytical calculations done here are in perfect agreement with the results obtained in* [4] (see Figure (3) in [4]). Thus we obtain that in the classical limit the ground state is given by the polarized orientation of dipoles. Moreover, we saw that in polarized (and also in striped) state the system has the $O(2)$ symmetry.

3.2.3 The Mean-field Approximation

Let us add the kinetic energy in this system. As mentioned numerous times in previous chapters each dipole will start to oscillate around its minimum energy orientation. Increasing the kinetic

energy, the oscillations will become stronger and at some point we will have to cross the quantum phase transition point. In order to investigate the phase transition, as it was done for the one-dimensional chain, let us first write the mean-field potential for the dipoles in triangular lattice. We will have:

$$\begin{aligned}
\langle\psi_{m,n}|\, V_{dd}^{i,j/i+m,j+n}\,|\psi_{m,n}\rangle &= \frac{C_{dd}}{8\pi}{\sum_{m,n}}' \frac{1}{|m^2+n^2+mn|^{3/2}} \\
&\times \Bigg\{ \cos(\theta_{i,j})\,\langle\psi_{m,n}|\cos(\theta_{i+m,j+n})\,|\psi_{m,n}\rangle \left(1-3\frac{\left(m+\frac{n}{2}\right)^2}{|m^2+n^2+mn|}\right) \\
&+ \sin(\theta_{i,j})\,\langle\psi_{m,n}|\sin(\theta_{i+m,j+n})\,|\psi_{m,n}\rangle \left(1-\frac{9}{4}\frac{n^2}{|m^2+n^2+mn|}\right) \\
&- \frac{3\sqrt{3}}{2}\frac{n\left(m+\frac{n}{2}\right)}{|m^2+n^2+mn|}\Big(\sin(\theta_{i,j})\,\langle\psi_{m,n}|\cos(\theta_{i+m,j+n})\,|\psi_{m,n}\rangle \\
&+ \cos(\theta_{i,j})\,\langle\psi_{m,n}|\sin(\theta_{i+m,j+n})\,|\psi_{m,n}\rangle \Big)\Bigg\} \quad . \qquad (3.56)
\end{aligned}$$

Knowing the minimum energy configuration for classical limit, and also knowing that the system in classical limit has $O(2)$ symmetry, we can assume that for any value of $\mathbf{m}$ and $\mathbf{n}$:

$$\sin(\theta_{i+m,j+n}) \to \langle\sin(\theta_{i+m,j+n})\rangle = 0 \quad \text{and} \quad \cos(\theta_{i+m,j+n}) \to \langle\cos(\theta_{i+m,j+n})\rangle = \Delta \quad . \qquad (3.57)$$

Plugging *eq.*(3.57) into *eq.*(3.42) we will obtain the full Hamiltonian of the system:

$$\begin{aligned}
\hat{H} &= -\frac{\hbar^2}{2I}\sum_{i,j}\frac{d^2}{d\theta_{i,j}^2} + \frac{C_{dd}}{8\pi}\sum_{i,j}{\sum_{m,n}}' \frac{\Delta}{|m^2+n^2+mn|^{3/2}}\Bigg\{\cos(\theta_{i,j}) \\
&\times\left(1-3\frac{\left(m+\frac{n}{2}\right)^2}{|m^2+n^2+mn|}\right) - \sin(\theta_{i,j})\frac{3\sqrt{3}}{2}\frac{n\left(m+\frac{n}{2}\right)}{|m^2+n^2+mn|}\Bigg\} \quad . \qquad (3.58)
\end{aligned}$$

It is obvious that, since the mean-field potential is written for a single dipole, we can decompose the total Hamiltonian of the system as a sum of individual Hamiltonians. Thus the Schrödinger equation for a single dipole **i,j** put into a mean-field will be as follows (from now on, we will remove index **i,j**):

$$\begin{aligned}
-\frac{\hbar^2}{2I}\frac{d^2}{d\theta^2}\psi(\theta) &+ \frac{C_{dd}}{8\pi}{\sum_{m,n}}' \frac{\Delta}{|m^2+n^2+mn|^{3/2}}\Bigg\{\cos(\theta)\left(1-3\frac{\left(m+\frac{n}{2}\right)^2}{|m^2+n^2+mn|}\right) \\
&- \sin(\theta)\frac{3\sqrt{3}}{2}\frac{n\left(m+\frac{n}{2}\right)}{|m^2+n^2+mn|}\Bigg\}\psi(\theta) = E\psi(\theta) \quad . \qquad (3.59)
\end{aligned}$$

Since we are again assuming that the system is in thermodynamic limit ($N \to \infty$), we will have:

$${\sum_{m,n}}' \frac{n\left(m+\frac{n}{2}\right)}{|m^2+n^2+mn|^{5/2}} = 0 \quad . \qquad (3.60)$$

Thus the Schrödinger equation can be simplified into the following:

$$-\frac{\hbar^2}{2I}\frac{d^2}{d\theta^2}\psi(\theta) - D\Delta\cos(\theta)\psi(\theta) = E\psi(\theta) \quad , \qquad (3.61)$$

where

$$D = \frac{C_{dd}}{8\pi}{\sum_{m,n}}' \frac{3\frac{\left(m+\frac{n}{2}\right)^2}{|m^2+n^2+mn|}-1}{|m^2+n^2+mn|^{3/2}} \quad . \qquad (3.62)$$

Schrödinger equation in *eq.*(3.61) can be re-written in the following way:

$$\frac{d^2}{d\eta^2}\psi(\eta) + \Big(\epsilon + 2q\cos(2\eta)\Big)\psi(\eta) = 0 \quad . \tag{3.63}$$

Here:

$$\epsilon = \frac{8IE}{\hbar^2} \quad \text{and} \quad q = \frac{4I}{\hbar^2}D\Delta \quad .$$

Thus again the Schrödinger equation for the single dipole in the mean-field is exactly the same as the equation for the one-dimensional system. Again the difference between these two equations is the parameter **D**. Because of this we can use the results obtained for the one-dimensional system and deduce: dipoles arranged in the triangular lattice in the weak interaction limit ($\mathbf{T} > \mathbf{V}$) will have the random orientation: $\Delta = \langle\cos(2\eta)\rangle = 0$, meaning that dipoles can be considered as *free*. In the strong interaction limit ($\mathbf{T} < \mathbf{V}$) dipoles are polarized: $\Delta = \langle\cos(2\eta)\rangle = 1$, also having the global $O(2)$ rotational symmetry. The quantum phase transition from highly disordered to polarized state happens when:

$$D_{crit} = \frac{\hbar^2}{I} \quad , \tag{3.64}$$

or when:

$$C_{dd}^{crit} = \frac{8\pi}{\beta}\frac{\hbar^2}{I} \quad \text{where} \quad \beta \approx 5.5 \quad . \tag{3.65}$$

Since the potential in the mean-field approximation is the same as in the one-dimensional system, the Hamiltonian for the system with six-fold potential $U(\theta)$ introduced in *eq.*(2.56) will have the same form (see *eq.*(2.66)). Hence the result made for the one-dimensional system will be the same for the triangular system:

$$D_{crit}^{new} > D_{crit}$$

3.3 Defects in Triangular Lattice

In the introduction, we said that the crystal lattice is ground in the chamber where there is a water vapor. This means that not every nano-cavity will house a water molecule. Having water vacancies in the system might alter the ground state configuration of the system leading to breaking of the ground state symmetry.

The question that needs to be answered is: what is the new order that will arise in the system after introducing the vacancy, and if a new configuration is formed will it change the symmetry of the system globally or locally.

In order to answer this questions let us do the following: let us assume that we have dipoles arranged in the honeycomb structure as shown in the figure (3.13). We assume that the central dipole is missing.

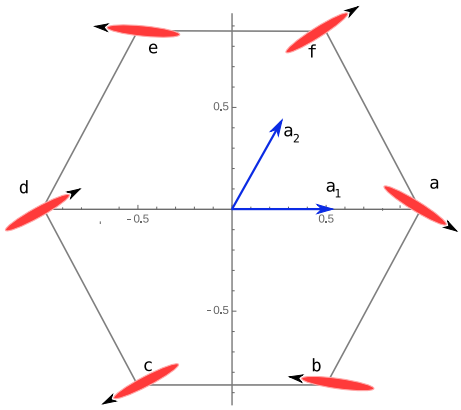

Figure 3.13: First honeycomb structure of dipolar lattice. The central dipole is missing. The dipole at coordinates $\{1, 0\}$ is called "a". The one below it is called "b" and the dipole above it is called "f". The dipole with the coordinates $\{-1, 0\}$ is called "d". The dipole bellow it is called "c" and the one above it is called "e".

In order to calculate the minimum energy configuration, we will write the interaction potential for all pairs of dipoles, assuming that dipoles have random orientation. Using the general form of the dipole-dipole interaction:

$$
\begin{aligned}
V_{dd}^{i,j/i+m,j+n} &= \frac{|d|^2}{4\pi\epsilon_0 a^3 |m^2+n^2+mn|^{3/2}} \\
&\times \Bigg\{ \cos(\theta_{i,j})\cos(\theta_{i+m,j+n})\left(1 - 3\frac{\left(m+\frac{n}{2}\right)^2}{|m^2+n^2+mn|}\right) \\
&+ \sin(\theta_{i,j})\sin(\theta_{i+m,j+n})\left(1 - \frac{9}{4}\frac{n^2}{|m^2+n^2+mn|}\right) \\
&- \frac{3\sqrt{3}}{2}\frac{n\left(m+\frac{n}{2}\right)}{|m^2+n^2+mn|}\Big(\sin(\theta_{i,j})\cos(\theta_{i+m,j+n}) \\
&+ \cos(\theta_{i,j})\sin(\theta_{i+m,j+n})\Big)\Bigg\} \quad , \qquad (3.66)
\end{aligned}
$$

we are able to write the total energy for the system. Minimizing the total energy with regards to six angles $\{\theta_a, \theta_b, \theta_c, \theta_d, \theta_e, \theta_f\}$, we were able to find the minimum energy configuration (for the full in-depth calculation see *Appendix* C). These configurations are depicted in the*Figure* (3.14). We found that the dipoles around the vacancy are forming the vortex configuration. It is crucial to notice that the dipoles have *two* ground state configurations: dipoles are aligned either clockwise

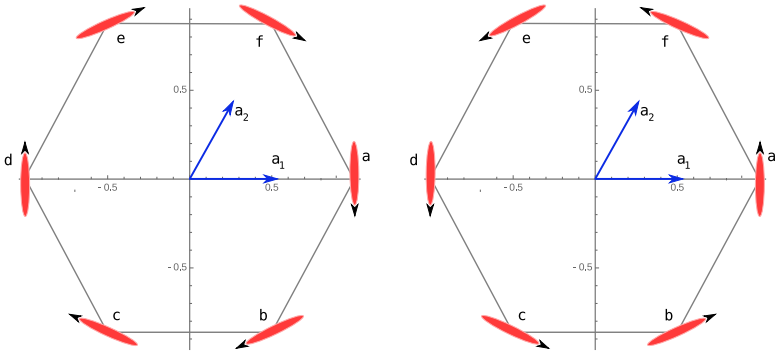

(a) Clockwise vortex (b) Counterclockwise vortex

Figure 3.14: Two ground state configurations for a honeycomb structure with a central dipole missing.

or counterclockwise. This means that we have a *spontaneous symmetry breaking*. Hence, around the missing dipole the global $O(2)$ symmetry is broken.

Let us try to generalize the obtained results for the whole system. In order to do this we again introduce the notion of the cutoff radius. As explained in the previous sections, the cutoff radius $\mathbf{r}_{cut}$ such that if the distance between two dipoles is greater than $\mathbf{r}_{cut}$, the interaction between them can be neglected. The mean-field approach, done in previous chapter, showed us that in ground state dipoles are polarized and have an $O(2)$ symmetry.

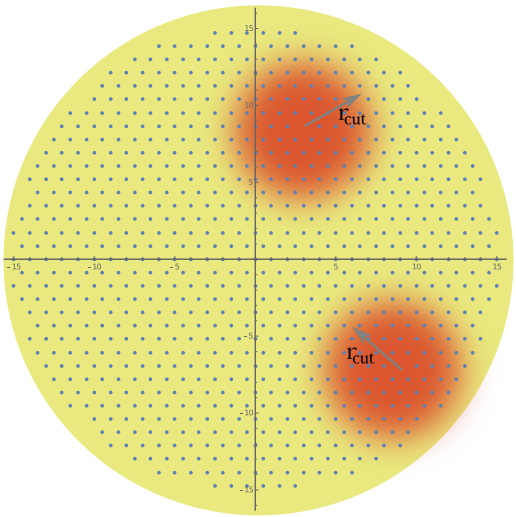

Figure 3.15: Triangular lattice of identical dipoles. Each dot represents a dipole (We do not show the dipole moment vector here). In the center of the blurred red circle we see that the dipole is missing. All dipoles around the vacancy inside the blurred red circle will have vortex configurations, but outside it (we have marked this place with yellow circle) every dipole will have a *polarized* configuration.

Hence, we can make the following assumption: the symmetry breaking introduced by the vacancy in the lattice is local: if we place a vacancy at the center of the circle with radius $\mathbf{r}_{cut}$ (see *Figure* (3.15)), we will see that every dipole in honeycomb structure inside the circle will have the vortex-like orientation, whereas all other dipoles living outside the circle will maintain their

polarized orientation.

Of course this is a very rough estimate. It is clear that we will not have a intersection *line*. We believe, that the line between the polarized and vortex configuration will be smeared out. In order to observe this one must do a *Monte-Carlo* simulation.

Knowing the properties of the two-dimensional systems, let us start our investigation of the three-dimensional crystal.

Chapter 4

Three-Dimensional Lattice of Water Molecules

Beryl, a mineral with the chemical formula: $Be_3Al_2Si_6O_{16}$, in general is a three-dimensional crystal. In the *Figure* (4.1a), taken from the paper [2], we see a horizontal cut of the beryl crystal. Mainly this cut is perpendicular to the crystallographic c-axis. We will remind the reader that the *yellow* triangles in the beryl crystal represent the SiO_4 molecules forming the honeycomb structure. These honeycomb structures sit on top of each other forming channels along c-axis. Water molecules, put inside these nano-cavities, form layers of the triangular lattice. *Figure* (4.1b) shows two such layers of triangular lattices put on top of each other. The distance between two layers is $r_{A,B} = \alpha$, where we have denoted the lower layer as **A** and the top layer as **B**.

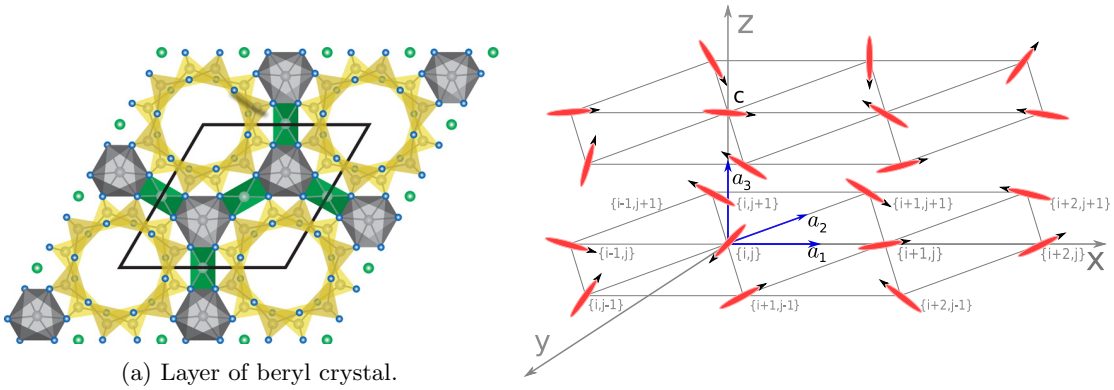

(a) Layer of beryl crystal.

(b) Two layers of triangular lattices.

Figure 4.1: The single layer of the beryl crystal (the cut is done perpendicular of c-axis) (a), and the schematic of three dimensional system: two layers of triangular lattice put one over another.

The distance between a dipole **c** situated in the layer **B** and any dipole **i+m,j+n** in the layer **A** can be written as follows:

$$\vec{r}_{c/m,n} = a\big(m\hat{a}_1 + n\hat{a}_2\big) - \alpha\hat{a}_3 \quad , \tag{4.1}$$

where unit vectors $\hat{a}_1, \hat{a}_2$, and $\hat{a}_2$ span the whole lattice (see *Figure* (4.1b)). The distance between neighboring dipoles in layer **A** is assumed to be equal to $\boldsymbol{a}$.

For the simplicity of upcoming derivations, let us write the general form of the dipole-dipole

interaction between dipoles **c** and **i+m,j+n**. We will have:

$$V_{dd}^{c/m,n} = \frac{C_{dd}}{4\pi|\alpha^2+a^2(m^2+n^2+mn)|^{3/2}}\left\{\vec{d}_c\cdot\vec{d}_{i+m,j+n} - 3\frac{(\vec{r}_{c/m,n}\cdot\vec{d}_c)\,(\vec{r}_{c/m,n}\cdot\vec{d}_{i+m,j+n})}{|\alpha^2+a^2(m^2+n^2+mn)|}\right\} \quad , \tag{4.2}$$

where $C_{dd} = |d|^2/\epsilon_0$ is a *coupling constant*. Writing down the scalar product for the second term in $V_{dd}^{c/m,n}$ we will obtain:

$$\vec{r}_{c/m,n}\cdot\vec{d}_c = a|d|\left\{\left(m+\frac{n}{2}\right)\cos(\theta_c)+\frac{\sqrt{3}}{2}n\sin(\theta_c)\right\} \quad , \tag{4.3}$$

where θ_c is the angle of the dipole $\vec{d}_c$ with x-axis.

We showed in the previous chapter that an individual layer of triangular lattice has a polarized configuration in the ground state. Moreover, such a system has a global $O(2)$ rotational symmetry. Hence, without loosing generality, we can assume that for any pairs of {**m, n**} in layer **A** (including $m = n = 0$):

$$\theta_{m,n} = 0 \quad , \tag{4.4}$$

where $\theta_{m,n}$ is the angle between the dipole moment of the dipole and the x-axis. In order to see how the dipole **c** in layer **B** aligns itself, let us picture the following situation. Picture a honeycomb structure in layer **A** and a single dipole in layer **B**. the schematic of such a system is shown in the *Figure* (4.2). In the layer **A** we have the following six dipoles (six following pairs of {**m, n**}):

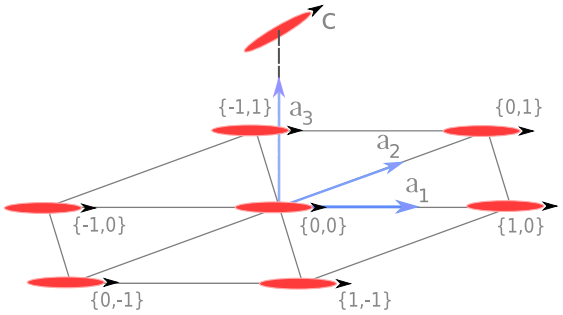

Figure 4.2: First honeycomb structure of dipolar lattice. We place one dipole **C** on top of the layer **A** of triangular lattice.

$$\{0,0\};\{1,0\};\{-1,0\};\{0,1\};\{-1,1\};\{0,-1\} \quad \text{and} \quad \{1,-1\} \quad . \tag{4.5}$$

We will calculate the total potential energy for dipole **c** interacting with the layer **A** assuming that layer is polarized along x-axis. Using*eq.*(4.2), we will obtain:

$$V_{dd}^{c} = \frac{C_{dd}}{4\pi}\sum_{m,n}\frac{1}{|\alpha^2+a^2(m^2+n^2+mn)|^{3/2}}\left\{\cos(\theta_c) - \frac{3a^2\left(m+\frac{n}{2}\right)}{|\alpha^2+a^2(m^2+n^2+mn)|}\left(\left(m+\frac{n}{2}\right)\cos(\theta_c)+\frac{\sqrt{3}}{2}n\sin(\theta_c)\right)\right\} \quad , \tag{4.6}$$

assuming that in the summation **m** and **n** take the values represented in *eq.*(4.5). Assuming that $\alpha = a = 1$, we will obtain:

$$V_{dd}^{c} = \frac{C_{dd}}{4\pi}\beta\cos(\theta_c), \quad \text{where} \quad \beta \approx 1.53 \quad . \tag{4.7}$$

Minimizing the potential for dipole **c** with regards to angle θ_c we see that the minimum is reached for:

$$\theta_c = \pi \quad . \tag{4.8}$$

It is obvious that adding more honeycomb structures in the layer **A** will *not* change the overall outcome for the dipole **c**: the dipole **c** will orient itself opposite of the orientation of layer **A**. Generalization of this finding for the total system is trivial. If two layers **A** and **B** are brought

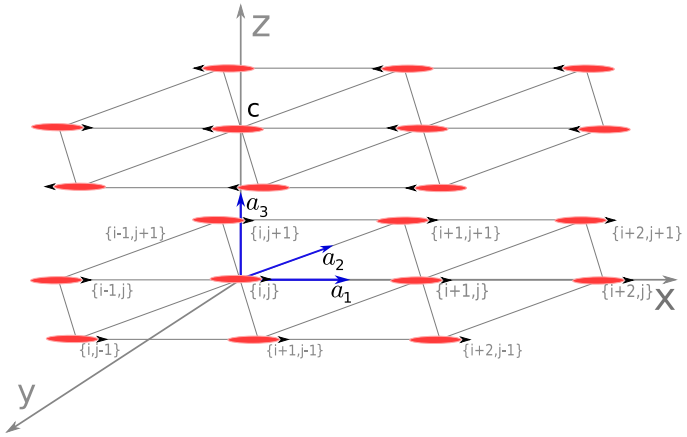

Figure 4.3: Ground state configuration of the three-dimensional system of dipoles (water molecules). We see that each layer has a polarized ordering. But the total three-dimensional system has a staggered configuration.

close together, they will be polarized in the opposite direction. For our case if the polarization angle ϕ of layer **A** is $\phi = 0$, then for layer **B** we will have: $\phi = \pi$ (see *Figure* (4.3)). Hence, we can declare that even though the individual layers have polarized configurations the total three dimensional system of dipoles has the *striped* configuration in its *ground state*.

Conclusion

In the coarse of the thesis, our main *goal* was to inspect the phase diagram of one, two and three-dimensional systems of water molecules, interacting with each other via a long-range dipole-dipole interaction, embedded in the nano-cavities of beryl crystal. Beryl, as mentioned numerously above, has nano-cavities created by the SiO_4 molecules, which can host single water molecules. In order to investigate the phase diagram we treated water molecules as *point particles having dipole moment*. Since the higher dimensional systems were complicated to inspect, we started our investigation with the *one-dimensional chain of identical dipoles*.

In the classical limit (*section* 2.1), we've obtained that dipoles form the polarized configuration along the z-axis (see *Figure* (2.3)): $\theta = 0$ (where θ is the angle between the dipole moment vector and z-axis). By increasing the kinetic energy of the system, we were able to find the critical value of the parameter $\mathbf{D}_{crit}$ (*section* 2.4), where the quantum phase transition occurs. We found: for $\mathbf{D} < \mathbf{D}_{crit}$ system choses the *highly disordered* state such that (*Figure* (2.9)):

$$\Delta = \langle \cos(\theta) \rangle = 0 \quad ,$$

meaning that every dipole orients itself randomly.

When $\mathbf{D} > \mathbf{D}_{crit}$ the system starts to arrange itself (*section* 2.5):

$$\Delta = \langle \cos(\theta) \rangle \neq 0 \quad \textit{and in classical limit} \quad \Delta = 1 \quad .$$

We have also observed, a symmetry breaking. In the weak interaction limit, when each individual water molecule can be considered as a free molecule, the system has both *local* and *global* $O(2)$ symmetry: rotation of the dipole moment vector of one molecule will not change the total energy of the system, and the global rotation of every dipole moment of every water molecule will also leave the system invariant.

In the experiment, as mentioned in previous, water molecules are put inside the honeycomb structure created by the SiO_4 molecules. In order to observe the changes of the phase diagram when the interaction between the water molecules (dipoles) and the SiO_4 molecules (six-fold potential) is increased, we used the *tight-binding* approach (*section* 2.6). Assuming that the mean-field potential (created by all dipoles in the system) is weaker than the six-fold potential, which we wrote as a sum of six individual Dirak-delta functions, we treated the mean-field potential as a perturbation (*section* 2.7). Using the perturbation theory, we were able to obtain the following: the overall phase diagram of water molecules remains the same: for weak ($\mathbf{T}>\mathbf{V}$) and strong ($\mathbf{T}<\mathbf{V}$) interaction limits the system behaves in the same manner as it did without the additional potential. The crucial finding was that the addition of the honeycomb structure *shifts* the quantum phase transition point. Mainly we found that:

$$D_{crit}^{new} > D_{crit} \quad .$$

Next, we discussed two-dimensional systems (***Chapter*** 3). In the beginning (*section* 3.1), we started with a *toy model*: quadratic lattice (*Figure* (3.2)) of individual dipoles and studied it's phase diagram. The approach to this problem was the same as for the one-dimensional chain. Initially, we assumed that the strength of the six-fold potential was weak enough that it's interaction between dipoles (water molecules) could have been neglected. In the classical limit (*section* 3.1), out of

three potential ground state configurations: polarized (*section* 3.1.1), striped (*section* 3.1.2) and checkerboard (*section* 3.1.3), we were able to obtain, that the *striped* configuration (*Figure* (3.6a)) had the lowest energy. In order to see the quantum phase transition we increased the kinetic energy. The dipoles started to oscillate around their energy minimum which lead to breaking of the ground state configuration. Here again, we used the mean-field approximation (*eq.* (3.22)) (taking into account the configuration obtained in the classical limit) to observe this phase transition from highly disordered to striped ordering. We obtained that the Schrödinger equation (*section* 3.1.4) for the square lattice (*eq.* (3.29)) had the same form as the one for the one-dimensional chain. The only difference was that the parameter **D** entering in both equations had to be redefined. Hence including the six-fold potential did not change the overall phase diagram: the critical value of **D** was shifted in the same manner as it was for the one-dimensional chain.

Beryl crystal suggests that water molecules form a triangular lattice. During the investigation of the triangular lattice (*Figure* (3.9)), initially we neglected the interaction between water molecules and the walls of the crystal (SiO_4). We found that two different configurations: polarized (*section* 3.2.1) and striped (*section* 3.2.2) have the potential to have the lowest energy. Writing down the general form of the dipole-dipole interaction (*eq.*(3.39)) (bearing in mind the geometry of the lattice) we compared the potential energies (per particle) for both configurations and obtained that the *polarized* configuration has the lowest energy. Moreover, we obtained that the system as the global $O(2)$ rotational symmetry in *ground state*. In order to see the phase transition, we allowed the kinetic energy to become stronger than the potential energy. Writing down the dipole-dipole interaction potential using the mean-field approximation (*eq.*(3.57)) (considering the configuration obtained in the classical limit) we arrived at the Schrödinger equation (*section* 3.2.3) which, surprisingly had the same form (*eq.*(3.63)) as the one for square lattice and one-dimensional chain. Again the difference was the definition of the parameter **D** entering the equation. This meant that overall phase diagram was the following: in the classical limit system was polarized and had the global $O(2)$ rotational symmetry. In the quantum mechanical limit ($\mathbf{T} > \mathbf{V}$) system was in *highly disordered* phase with local (and global) $O(2)$ symmetry.

We were also interested to observe the change of the global properties of the system (for triangular lattice) when a deficiency of water molecules was introduced. In order to see how the system of dipoles would react (either globally or locally) to a deficiency we did the following (*section* 3.3): we removed a dipole randomly and probed the ordering created around the deficiency point. We obtained that the nearest six dipoles, which formed the honeycomb structure, gave the vortex like configuration in the ground state (*Figure* (3.14)). The vortexes had either clockwise or counterclockwise direction, indicating the existence of the *spontaneous symmetry breaking*. We argued that the breaking of the global $O(2)$ symmetry is local: The overall system will maintain the polarized configuration (with $O(2)$ symmetry), but we will see *islands* of vortex configurations forming around deficiency points (*Figure* (3.15)).

Finally, as an interest we explored the three dimensional system of water molecules (***Chapter*** 4). We obtained that two nearest neighboring layers of dipoles, forming triangular lattices are polarized in the opposite direction (*Figure* (4.2)): if one layer has a polarization $\phi = 0$, the neighbor layer will have polarization $\phi = \pi$. Hence, we declared that even though the individual layers have polarized configurations the total three dimensional system of dipoles has the *striped* configuration in its *ground state*.

Outlook

As it turned out, water molecules show an interesting behavior when placed in nano-cavities (in our case in the beryl crystal). But, we argue that there is much to learn from this system.

In this thesis we have always assumed that the system is infinite (in the thermodynamic limit), but the reality is, that the beryl crystal is finite. Knowing the bulk properties of such system the next obvious question is: what will happen, how the water molecules will be have at the borders of the crystal.

there is another topic that was not discussed in this thesis. Imagine that you that you have a sample that is heated at some temperature **T** (assume that at this temperature water molecules are free). If one cools down the system, one might see domains having different configurations. It is interesting to research what is happening at the intersection of these domains.

These are the topics that we leave for the future research.

Appendices

Appendix A

Self-consistent equation for intermediate values of "q"

Let us rewrite again the Mathieu equation that we had in *eq.*(2.25):

$$\frac{d^2}{d\eta^2}\psi(\eta) + \Big(\epsilon + 2q\cos(2\eta)\Big)\psi(\eta) = 0 \quad . \tag{A.1}$$

Here, again, ϵ is the energy eigenvalue and $\mathbf{q}$ is a self-consistent parameter defined as:

$$q = \frac{4ID}{\hbar^2}\Delta \quad \text{where} \quad \Delta = \langle\cos(2\eta)\rangle \tag{A.2}$$

We saw in [5], that the wave-function for the ground state looks like:

$$\psi_0(\theta) = \frac{1}{\sqrt{\pi}}\sum_{k=0}^{\infty} A_{2k}^{(0)}\cos\Big(k(\pi-\theta)\Big) \tag{A.3}$$

where $\theta = 2\eta$. Here we give a full in-depth derivation of $\langle\cos(2\eta)\rangle$.

So let us begin:

$$\begin{aligned}\langle\psi_0|\cos(\theta)|\psi_0\rangle \quad &= \frac{1}{\pi}\sum_{k=0}^{\infty}\sum_{l=0}^{\infty} A_{2k}^{(0)}A_{2l}^{(0)}\int_0^{2\pi} d\theta\cos(\theta)\cos\big(k(\pi-\theta)\big)\cos\big(l(\pi-\theta)\big) \\ &= \frac{1}{\pi}\sum_{k=0}^{\infty}\sum_{l=0}^{\infty}(-1)^{k+l}A_{2k}^{(0)}A_{2l}^{(0)}\int_0^{2\pi} d\theta\cos\big(\theta\big)\cos\big(k\theta\big)\cos\big(l\theta\big) \quad .\end{aligned} \tag{A.4}$$

Using the identity property of the trigonometric functions, we will obtain:

$$\int_0^{2\pi} d\theta\cos\big(\theta\big)\cos\big(k\theta\big)\cos\big(l\theta\big) = \frac{1}{2}\left\{\frac{(k-l)\sin\big(2\pi(k-l)\big)}{(k-l)^2-1} + \frac{(k+l)\sin\big(2\pi(k+l)\big)}{(k+l)^2-1}\right\} \tag{A.5}$$

Let us calculate the value of *eq.*(A.5) for $k = 0$ and $l = 1$. We will have:

$$\int_0^{2\pi} d\theta\cos\big(\theta\big)\cos\big(k\theta\big)\cos\big(l\theta\big)\Big|_{k=0}^{l=1} = \frac{l\sin\big(2\pi l\big)}{l^2-1}\Big|_{l=1} \quad . \tag{A.6}$$

Notice that for $l = 1$ the nominator and the denominator in *eq.*(A.6) are zero. Thus we have to use the L'Hôpital's rule to calculate it. As a short reminder L'Hôpital's rule can be written as:

$$\lim_{x\to c}\frac{f(x)}{g(x)} = \lim_{x\to c}\frac{f'(x)}{g'(x)} \quad \text{if} \quad \lim_{x\to c} f(x) = \lim_{x\to c} g(x) = 0 \text{ or } \pm\infty \quad . \tag{A.7}$$

Thus, we will have:

$$\left.\frac{l\sin\left(2\pi l\right)}{l^2-1}\right|_{l=1} = \pi \quad \rightarrow \quad \left.\int_0^{2\pi} d\theta \cos\left(\theta\right)\cos\left(k\theta\right)\cos\left(l\theta\right)\right|_{k=0}^{l=1} = \pi \quad . \tag{A.8}$$

It is clear that for $k=1, l=0$ we will have the same result. For $k=l=1$ and $k=l=0$ from *eq.*(A.5) we will obtain that:

$$\int_0^{2\pi} d\theta \cos\left(\theta\right)\cos^2\left(k\theta\right) = 0 \tag{A.9}$$

Using *eq.*(A.8) and *eq.*(A.9), we can write the result of the integral in a matrix form.

$$\left.\int_0^{2\pi} d\theta \cos\left(\theta\right)\cos\left(k\theta\right)\cos\left(l\theta\right)\right|_{k=0}^{l=1} = \begin{pmatrix} 0 & \pi \\ \pi & 0 \end{pmatrix} \tag{A.10}$$

For $k=1, l=2$ (or vise versa), using the identity property of trigonometric functions, we will have:

$$\left.\int_0^{2\pi} d\theta \cos\left(\theta\right)\cos\left(k\theta\right)\cos\left(l\theta\right)\right|_{k=1}^{l=2} = \frac{\pi}{2} \tag{A.11}$$

Thus we can write a general result of the integral in the following matrix form:

$$\int_0^{2\pi} d\theta \cos\left(\theta\right)\cos\left(k\theta\right)\cos\left(l\theta\right) = \begin{pmatrix} 0 & \pi & 0 & 0 & 0 & \dots \\ \pi & 0 & \pi/2 & 0 & 0 & \dots \\ 0 & \pi/2 & 0 & \pi/2 & 0 & \dots \\ 0 & 0 & \pi/2 & 0 & \pi/2 & \dots \\ 0 & 0 & 0 & \pi/2 & 0 & \dots \\ . & . & . & . & . & . \end{pmatrix} \quad . \tag{A.12}$$

It is clear from *eq.*(A.12) that only those values of k for which $k=l-1$ (where $l>1$) we will have a nonzero value. Because of this one can make a simplification to *eq.*(A.12), and write it in

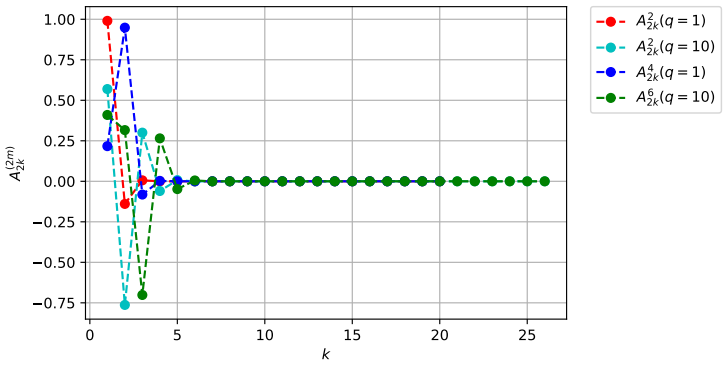

Figure A.1: Coefficients $A_{2k}^{(2m)}$ calculated for $m=\{1,2,3\}$ and $q=\{1,10\}$ as a function of summation variable k. One can see that for $k>5$ $A_{2k}^{(2m)} \approx 0$.

the following way:

$$\int_0^{2\pi} d\theta \cos\left(\theta\right)\cos\left((l-1)\theta\right)\cos\left(l\theta\right) = \left(\pi;\quad \pi/2;\quad \pi/2;\quad \pi/2;\quad \dots\right) \quad . \tag{A.13}$$

Plugging this into *eq.*(A.4), we will obtain the following result for the $\langle\cos(\theta)\rangle$:

$$\langle\psi_0|\cos(\theta)|\psi_0\rangle = \left(A_0^{(0)}\right)^2 + \frac{1}{2}\sum_{l=2}^{\infty}(-1)^{2l-1}A_{2(l-1)}^{(0)}A_{2l}^{(0)} \quad . \tag{A.14}$$

Now using the notations introduced in *eq.*(A.2) we will obtain:

$$\frac{\hbar^2}{4ID}q = \left(A_0^{(0)}\right)^2 + \frac{1}{2}\sum_{l=2}^{\infty}(-1)^{2l-1}A_{2(l-1)}^{(0)}A_{2l}^{(0)} \quad . \tag{A.15}$$

Notice that A is a function of $\mathbf{q}$. *Eq.*(A.15) is a self-consistent equation for $\mathbf{q}$. It is unfortunate that this equation can not be solved analytically, since there is no definite form of the coefficients A. But one can successfully solve this equation using numeric methods.

One might say that since the summation goes to infinity there is no possible way to solve *eq.*(A.15). This is not true, since the coefficient A decays rapidly as the value of l is increased (see *Figure* (A.1)).

Appendix B

Riemann zeta function

The Riemann zeta function can be defined by the following integral:

$$\zeta(x) = \frac{1}{\Gamma(x)} \int_0^\infty \frac{u^{x-1}}{e^u - 1} du \quad , \tag{B.1}$$

where $\Gamma(x)$ is the Gamma function. The Gamma function can also be represented using the following integral:

$$\Gamma(x) = \int_0^\infty e^{-z} z^{x-1} dy \quad . \tag{B.2}$$

Assuming that x in eq.(B.1) is an integer, we can re-write the integrand. We will have:

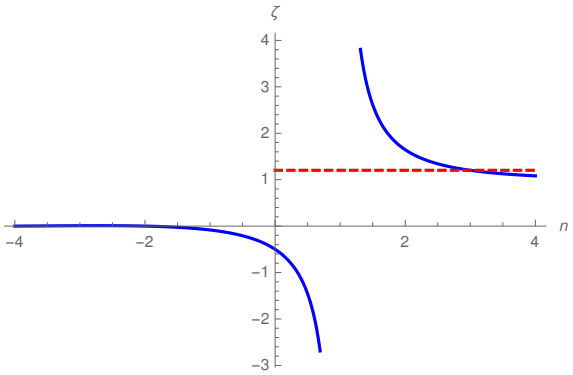

Figure B.1: Riemann zeta function $\zeta(n)$ as a function of n (blue continues line). The red dashed line represents $\zeta(3)$.

$$\frac{u^{x-1}}{e^u - 1} = e^{-u} \frac{u^{x-1}}{1 - e^{-u}} = e^{-u} u^{x-1} \sum_{k=0}^{\infty} e^{-ku} = u^{x-1} \sum_{k=1}^{\infty} e^{-ku} \quad . \tag{B.3}$$

Plugging this into eq.(B.1) we will obtain:

$$\zeta(x) = \frac{1}{\Gamma(x)} \sum_{k=1}^{\infty} \int_0^\infty e^{-ku} u^{x-1} du \quad . \tag{B.4}$$

Using the following notation:

$$u = \frac{y}{k} \quad , \tag{B.5}$$

we will obtain:

$$\zeta(x) = \frac{1}{\Gamma(x)} \sum_{k=1}^{\infty} \frac{1}{k^x} \int_0^{\infty} e^{-y} y^{x-1} dy = \sum_{k=1}^{\infty} \frac{1}{k^x} \quad . \tag{B.6}$$

Here we used eq.(B.2). Thus we obtained that for x being an integer the zeta function can be written as:

$$\zeta(n) = \sum_{k=1}^{\infty} \frac{1}{k^n} \tag{B.7}$$

In the figure (B.1) we show with the blue lines the $\zeta(n)$ as a function of n. The red dotted strait line represents $\zeta(3)$.

Using eq.(B.7) we can re-write the potential for a dipole in classical limit. Using eq.(2.13) we will have:

$$V_{dd}^0 = -\frac{C_{dd}}{\pi a^3} \sum_{j=1}^{\infty} \frac{1}{j^3} = -\frac{C_{dd}}{\pi a^3} \zeta(3) \approx -1.2 \frac{C_{dd}}{\pi a^3} \tag{B.8}$$

Appendix C

triangular lattice of dipoles with one dipole missing

In order to see how the system will react to introduction of a defect, let us do the following. In the figure (C.1) we can see dipoles arranged on honeycomb structure. We can also observe that the central dipole is missing. We will calculate the total energy of this system assuming that dipoles are randomly oriented. After writing the total energy, we will minimize it with respect to angles $\{\theta_a, \theta_b, \theta_c, \theta_d, \theta_e, \theta_f\}$.

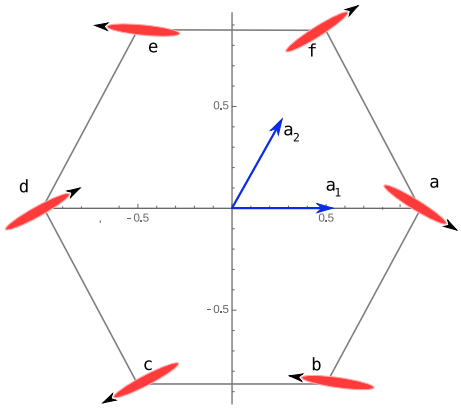

Figure C.1: First honeycomb structure of dipolar lattice. The central dipole is missing. The dipole at coordinates $\{1, 0\}$ is called "a". The one below it is called "b" and the dipole above it is called "f". The dipole with the coordinates $\{-1, 0\}$ is called "d". The dipole bellow it is called "c" and the one above it is called "e".

In the figure (C.1) we have unit vectors $\hat{a}_1$ and $\hat{a}_2$, such that:

$$\hat{a}_1 \cdot \hat{a}_2 = \frac{1}{2}$$

For the reader, we will write the general form of the dipole-dipole interaction:

$$\begin{aligned} V_{dd}^{i,j/i+m,j+n} &= \frac{|d|^2}{4\pi\epsilon_0 a^3 |m^2+n^2+mn|^{3/2}} \\ &\times \Bigg\{ \cos(\theta_{i,j})\cos(\theta_{i+m,j+n})\left(1-3\frac{\left(m+\frac{n}{2}\right)^2}{|m^2+n^2+mn|}\right) \\ &+ \sin(\theta_{i,j})\sin(\theta_{i+m,j+n})\left(1-\frac{9}{4}\frac{n^2}{|m^2+n^2+mn|}\right) \\ &- \frac{3\sqrt{3}}{2}\frac{n\left(m+\frac{n}{2}\right)}{|m^2+n^2+mn|}\Big(\sin(\theta_{i,j})\cos(\theta_{i+m,j+n}) \\ &+ \cos(\theta_{i,j})\sin(\theta_{i+m,j+n})\Big)\Bigg\} \quad . \end{aligned} \tag{C.1}$$

Using this we can start writing interactions between pairs of dipoles. We will have:

$$V_{dd}^{d-a} = \frac{|d|^2}{4\pi\epsilon_0 a^3}\frac{1}{8}\Big(\sin\theta_d \sin\theta_a - 2\cos\theta_d\cos\theta_a\Big) \tag{C.2}$$

$$\begin{aligned} V_{dd}^{d-b} &= \frac{|d|^2}{4\pi\epsilon_0 a^3}\frac{1}{3\sqrt{3}}\Big(\cos\theta_d\cos\theta_b + \sin\theta_d\sin\theta_b - \frac{1}{4}\Big(3\cos\theta_d - \sqrt{3}\sin\theta_d\Big) \\ &\times\Big(3\cos\theta_b - \sqrt{3}\sin\theta_b\Big)\Big) \end{aligned} \tag{C.3}$$

$$\begin{aligned} V_{dd}^{d-c} &= \frac{|d|^2}{4\pi\epsilon_0 a^3}\Big(\cos\theta_d\cos\theta_c + \sin\theta_d\sin\theta_c - \frac{3}{4}\Big(\cos\theta_d - \sqrt{3}\sin\theta_d\Big) \\ &\times\Big(\cos\theta_c - \sqrt{3}\sin\theta_c\Big)\Big) \end{aligned} \tag{C.4}$$

$$\begin{aligned} V_{dd}^{d-e} &= \frac{|d|^2}{4\pi\epsilon_0 a^3}\Big(\cos\theta_d\cos\theta_e + \sin\theta_d\sin\theta_e - \frac{3}{4}\Big(\cos\theta_d + \sqrt{3}\sin\theta_d\Big) \\ &\times\Big(\cos\theta_e + \sqrt{3}\sin\theta_e\Big)\Big) \end{aligned} \tag{C.5}$$

$$\begin{aligned} V_{dd}^{d-f} &= \frac{|d|^2}{4\pi\epsilon_0 a^3}\frac{1}{3\sqrt{3}}\Big(\cos\theta_d\cos\theta_f + \sin\theta_d\sin\theta_f - \frac{1}{4}\Big(3\cos\theta_d + \sqrt{3}\sin\theta_d\Big) \\ &\times\Big(3\cos\theta_f + \sqrt{3}\sin\theta_f\Big)\Big) \end{aligned} \tag{C.6}$$

$$V_{dd}^{e-f} = \frac{|d|^2}{4\pi\epsilon_0 a^3}\Big(\sin\theta_f\sin\theta_e - 2\cos\theta_f\cos\theta_e\Big) \tag{C.7}$$

$$\begin{aligned} V_{dd}^{e-a} &= \frac{|d|^2}{4\pi\epsilon_0 a^3}\frac{1}{3\sqrt{3}}\Big(\cos\theta_e\cos\theta_a + \sin\theta_e\sin\theta_a - \frac{1}{4}\Big(3\cos\theta_e - \sqrt{3}\sin\theta_e\Big) \\ &\times\Big(3\cos\theta_a - \sqrt{3}\sin\theta_a\Big)\Big) \end{aligned} \tag{C.8}$$

$$\begin{aligned} V_{dd}^{e-b} &= \frac{|d|^2}{4\pi\epsilon_0 a^3}\frac{1}{8}\Big(\cos\theta_e\cos\theta_b + \sin\theta_e\sin\theta_b - \frac{3}{4}\Big(\cos\theta_e - \sqrt{3}\sin\theta_e\Big) \\ &\times\Big(\cos\theta_b - \sqrt{3}\sin\theta_b\Big)\Big) \end{aligned} \tag{C.9}$$

$$V_{dd}^{e-c} = \frac{|d|^2}{4\pi\epsilon_0 a^3}\frac{1}{3\sqrt{3}}\Big(\sin\theta_e \sin\theta_c - 2\cos\theta_e\cos\theta_c\Big) \tag{C.10}$$

$$\begin{aligned} V_{dd}^{f-a} &= \frac{|d|^2}{4\pi\epsilon_0 a^3}\Big(\cos\theta_f\cos\theta_a + \sin\theta_f\sin\theta_a - \frac{3}{4}\Big(\cos\theta_f - \sqrt{3}\sin\theta_f\Big) \\ &\quad\times\Big(\cos\theta_a - \sqrt{3}\sin\theta_a\Big)\Big) \end{aligned} \tag{C.11}$$

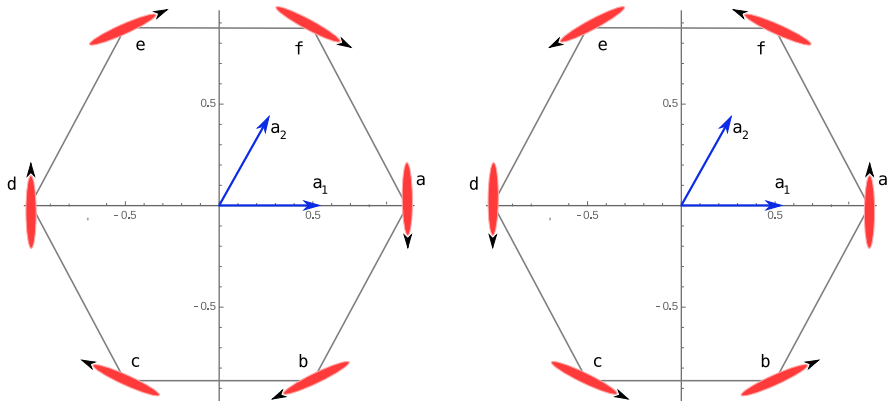

(a) Clockwise vortex (b) Counterclockwise vortex

Figure C.2: Two ground state configurations for a honeycomb structure with a central dipole missing.

$$V_{dd}^{f-b} = \frac{|d|^2}{4\pi\epsilon_0 a^3}\frac{1}{3\sqrt{3}}\Big(\cos\theta_f\cos\theta_b - 2\sin\theta_f\sin\theta_b\Big) \tag{C.12}$$

$$\begin{aligned} V_{dd}^{f-c} &= \frac{|d|^2}{4\pi\epsilon_0 a^3}\frac{1}{8}\Big(\cos\theta_f\cos\theta_c + \sin\theta_f\sin\theta_c - \frac{3}{4}\Big(\cos\theta_f + \sqrt{3}\sin\theta_f\Big) \\ &\quad\times\Big(\cos\theta_c + \sqrt{3}\sin\theta_c\Big)\Big) \end{aligned} \tag{C.13}$$

$$\begin{aligned} V_{dd}^{a-b} &= \frac{|d|^2}{4\pi\epsilon_0 a^3}\Big(\cos\theta_a\cos\theta_b + \sin\theta_a\sin\theta_b - \frac{3}{4}\Big(\cos\theta_a + \sqrt{3}\sin\theta_a\Big) \\ &\quad\times\Big(\cos\theta_b + \sqrt{3}\sin\theta_b\Big)\Big) \end{aligned} \tag{C.14}$$

$$\begin{aligned} V_{dd}^{a-c} &= \frac{|d|^2}{4\pi\epsilon_0 a^3}\frac{1}{3\sqrt{3}}\Big(\cos\theta_a\cos\theta_c + \sin\theta_a\sin\theta_c - \frac{1}{4}\Big(3\cos\theta_a + \sqrt{3}\sin\theta_a\Big) \\ &\quad\times\Big(3\cos\theta_c + \sqrt{3}\sin\theta_c\Big)\Big) \end{aligned} \tag{C.15}$$

$$V_{dd}^{b-c} = \frac{|d|^2}{4\pi\epsilon_0 a^3}\Big(\sin\theta_b\sin\theta_c - 2\cos\theta_b\cos\theta_c\Big) \tag{C.16}$$

The total energy of the system will be the sum of interactions through equations (C.2) - (C.16). The minimization of the tota energy with regards to the six angles is done using "Mathematica". The final results are shown in the figure (C.2). We can observe that around the vacancy point the dipoles form either clockwise vortex-like orientation or counterclockwise vortex-like orientation. It is worthwhile to notice that we have the spontaneous symmetry breaking.

Appendix D

One-Dimensional Chain of Dipoles

Let us assume, that we have a chain of identical dipoles polarized along z-axis. We make a following change in the system: we flip the dipole m such that: $\theta_m = \pi$. From the Chapter, where we discussed one-dimensional chain of dipoles, we know that if two dipoles - m and j - are parallel to each other, the interaction between them can be written in the following way:

$$V_{dd}^{m,j} = -\frac{|d|^2}{2\pi\epsilon_0 a^3}\frac{1}{|j-m|^3} \quad . \tag{D.1}$$

If these two dipoles are anti-parallel to each other - $\theta_j = \theta_m + \pi$ - the interaction will be:

$$V_{dd}^{m,j} = \frac{|d|^2}{2\pi\epsilon_0 a^3}\frac{1}{|j-m|^3} \quad . \tag{D.2}$$

Potential felt by dipole m (which is flipped) can be written as follows:

$$V_{dd}^{'} = \frac{|d|^2}{2\pi\epsilon_0 a^3}\sum_{j}^{N\,'}\frac{1}{|j-m|^3} \quad , \tag{D.3}$$

where the apostrophe in the summation means that we do not take into account the term $j = m$. Since we are in the thermodynamic limit - $N \to \infty$ - we can choose $m = 0$, and argue that the result will be the same for any m. Thus eq.(D.3) can be rewritten as follows:

$$V_{dd}^{'} = \frac{|d|^2}{2\pi\epsilon_0 a^3}\sum_{j}^{\,'}\frac{1}{|j|^3} = \frac{|d|^2}{\pi\epsilon_0 a^3}\sum_{j>0}\frac{1}{|j|^3} \quad . \tag{D.4}$$

The energy difference between this and the polarized configuration will be:

$$\Delta V = V_{dd}^{'} - V_{dd}^{Pol} = 2\frac{|d|^2}{\pi\epsilon_0 a^3}\sum_{j>0}\frac{1}{|j|^3} = 2\frac{|d|^2}{\pi\epsilon_0 a^3}\zeta(3) \quad , \tag{D.5}$$

where $\zeta(n)$ is the Riemann zeta function discussed in Appendix B. Let us flip a second dipole: the one next to $m = 0$. Then the total interaction will be:

$$V_{dd}^{'} = \frac{|d|^2}{2\pi\epsilon_0 a^3}\left(\sum_{j=-N}^{-1}\frac{1}{|j|^3} + \sum_{j=2}^{N}\frac{1}{j^3} - 1\right) \quad , \tag{D.6}$$

where first term is the total interaction between dipole $m = 0$ and any other dipole left to it, the second term is the interaction between the same dipole and all dipoles on the right apart from dipole $m = 1$, which is given in the third term. In general having n dipoles flipped in the system, the total potential for dipole $m = 0$ will be:

$$V_{dd}^{Tot} = \frac{|d|^2}{2\pi\epsilon_0 a^3}\left(\sum_{j=1}^{N}\frac{1}{j^3} + \sum_{j=n}^{N}\frac{1}{j^3} - \sum_{j=1}^{n}\frac{1}{j^3}\right) \quad , \tag{D.7}$$

where we used the following:

$$\sum_{j=-N}^{-1} \frac{1}{|j|^3} = \sum_{j=1}^{N} \frac{1}{j^3}$$

Rewriting the sums in eq.(D.7), we will obtain:

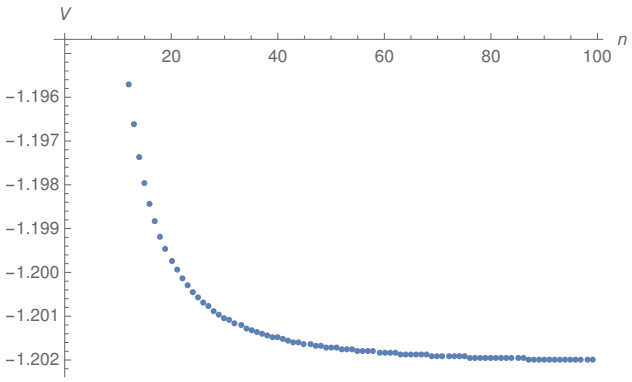

Figure D.1: V_{dd}^{Tot} as a function of n for fixed value of N: $N = 100$.

$$V_{dd}^{Tot} = 2\Big(-\sum_{j=1}^{N} \frac{1}{j^3} + \sum_{j=n+1}^{n} \frac{1}{j^3} \Big) \tag{D.8}$$

Bibliography

[1] Ruth M. Lynden-Bell, Simon C. Morris, John D. Barrow, John L. Finney and Charles L. Harper, JR. *Water and Life*. **2010**.

[2] Boris P. Gorshunov, Elena S. Zhukova, Victor I. Torgashev, Vladimir V. Lebedev, Gil'man S. Shakurov, Reinhard K. Kremer, Efim V. Pestrjakov, Victor G. Thomas, Dimitry A. Fursenko, and Martin Dressel. *Quantum Behavior of Water Molecules Confined to Nanocavities in Gemstones*. J. Phys. Chem. Lett., **2013**, 4 (12), pp 2015 - 2020.

[3] Boris Koselov. *Vibrational States of* H_2O *in Beryl: Physical Aspects*. Phys. Chem. Minerals, **2008**, 34, pp 271 - 278.

[4] Brendan P. Abolins, Robert E. Zillich,K. Birgitta Whaley. *Quantum Phases of Dipolar Rotors on Two-dimensional Lattice*. J. Chem. Phys. 148, 102338 **2018**.

[5] M. Abramowitz and Irene A. Stegun. *Handbook of Mathematical Functions*. Issue year: **1964**, pp 721 - 726.

[6] I.S. Gradshteyn and I.M. Stegun. *Table of Integrals, Series, and Products*. Issue year: **1963**, pp 991 - 993.